Article

Immobilization and Release Studies of Triazole Derivatives from Grafted Copolymer Based on Gellan-Carrying Betaine Units

Nicolae Baranov [1,2]**, Stefania Racovita** [3]**, Silvia Vasiliu** [3,*]**, Ana Maria Macsim** [3] **, Catalina Lionte** [4]**, Valeriu Sunel** [2]**, Marcel Popa** [1,5,*] **, Jacques Desbrieres** [6] **and Corina Cheptea** [7]

[1] Department of Natural and Synthetic Polymers, Faculty of Chemical Engineering and Environmental Protection, Gheorghe Asachi Technical University of Iasi, Prof. Dr. Docent Dimitrie Mangeron Street, No. 73, 700050 Iasi, Romania; Baranov_nicolae@yahoo.com

[2] Faculty of Chemistry, Al. I. Cuza University, Carol I Bvd., No. 11, 700506 Iasi, Romania; vsunel@uaic.ro

[3] Department of "Mihai Dima" Functional Polymers, Petru Poni Institute of Macromolecular Chemistry, Grigore Ghica Voda Alley, No. 41A, 700487 Iasi, Romania; stefania.racovita@icmpp.ro (S.R.); macsim.ana@icmpp.ro (A.M.M.)

[4] Faculty of Medicine, Gr. T. Popa University of Medicine and Pharmacy, Universitatii Street, No. 16, 700115 Iasi, Romania; clionte@yahoo.com

[5] Academy of Romanian Scientists, Splaiul Independentei Street No. 54, 050085 Bucuresti, Romania

[6] Institut des Sciences Analytiques et de Physico-Chimie pour l'Environnement et les Materiaux (IPREM), Pau and Pays de l'Adour University (UPPA), UMR CNRS 5254, Helioparc Pau Pyrenees, 2 av. President Angot, CEDEX 09, 64053 Pau, France; jacques.desbrieres@univ-pau.fr

[7] Department of Biomedical Sciences, Faculty of Biomedical Bioengineering, Gr. T. Popa University of Medicine and Pharmacy, Kogalniceanu Street No. 9–13, 700454 Iasi, Romania; coricheptea@yahoo.com

* Correspondence: silvia.vasiliu@icmpp.ro (S.V.); marpopa2001@yahoo.fr (M.P.)

Abstract: New polymer-bioactive compound systems were obtained by immobilization of triazole derivatives onto grafted copolymers and grafted copolymers carrying betaine units based on gellan and N-vinylimidazole. For preparation of bioactive compound, two new types of heterocyclic thio-derivatives with different substituents were combined in a single molecule to increase the selectivity of the biological action. The 5-aryl-amino-1,3,4 thiadiazole and 5-mercapto-1,2,4-triazole derivatives, each containing 2-mercapto-benzoxazole nucleus, were prepared by an intramolecular cyclization of thiosemicarbazides-1,4 disubstituted in acidic and basic medium. The structures of the new bioactive compounds were confirmed by elemental and spectral analysis (FT-IR and ^{1}H-NMR). The antimicrobial activity of 1,3,4 thiadiazoles and 1,2,4 triazoles was tested on gram-positive and gram-negative bacteria. The triazole compound was chosen to be immobilized onto polymeric particles by adsorption. The Langmuir, Freundlich, and Dubinin–Radushkevich adsorption isotherm were used to describe the adsorption equilibrium. Also, the pseudo-first and pseudo-second models were used to elucidate the adsorption mechanism of triazole onto grafted copolymer based on N-vinylimidazole and gellan (PG copolymer) and grafted copolymers carrying betaine units (PGB1 copolymer). In vitro release studies have shown that the release mechanism of triazole from PG and PGB1 copolymers is characteristic of an anomalous transport mechanism.

Keywords: grafted copolymer; triazole derivative; adsorption studies

1. Introduction

The design of new bioactive compounds that can be immobilized onto a polymeric support to achieve a controlled/sustained release and to find a way to treat some diseases represents an important goal in medical and pharmaceutical research [1,2].

Depending on the radicals present on the heterocycle, the organic compounds that contain in their molecule 1,3,4-thiadiazole and 1,2,4-triazole heterocycles have gained a remarkable interest due to their different biological properties, such as: antibacterial [3–5],

antifungal [6–9], tuberculostatic [10,11], analgesic [12,13], anti-inflammatory [14,15], hypnotic and sedative [16], cardioprotective [17], anticancer [18–22], anti-ulcerative [23], anticonvulsant [24], antidiabetic agents [25], allosteric modulators [26], and cathepsin B and tubulin inhibitors [27,28].

At the same time, the addition of a benzoxazole structure can be useful for the improvement of the biological activity. An argument in favor of this statement is that the compounds with benzoxazole heterocycle in their structure have practically the same biological properties like thiadiazole and triazole derivatives, such as antimicrobial, antifungal, antiviral, anti-inflammatory, antipyretic, analgesic, anticonvulsant, tuberculostatic, and antitumor agents [29–36]. Benzoxazole and triazole heterocyclic rings played an important role in the improving of antimicrobial and anticancer activity of the bioactive compounds [37].

These facts served as an argument in the synthesis of new heterocyclic compounds containing 1,3,4-thiadiazole and 1,2,4-triazole nucleus and the rest of 2-mercaptobenzoxazole, considering their mutual influence as well as the biological effect that can be generated throughout the molecule.

Although the researches on compounds with a benzoxazole structure are multiple and varied [38–41], some aspects of the synthesis and studies of these types of compounds in which both thiadiazole and triazole structures are grafted on the aromatic heterocycle, 2-mercaptobenzoxazole, have not been studied. Based on this premise, we expanded our research to the synthesis of new derivatives of 1,3,4-thiadiazole and 1,2,4-triazole classes of compounds using 1,4-disubstituted thiosemicarbazides as intermediates.

Also, the choice of macromolecular support for immobilization of bioactive compounds is very important. Encouraged by the preliminary results obtained in our previous study [42], we chose to use for the immobilization of these new bioactive compounds two types of macromolecular supports: grafted copolymers and grafted copolymers carrying betaine units based on gellan and N-vinylimidazole (PG and PGB1, respectively). The structure of PG and PGB1 copolymers are presented in Figure 1.
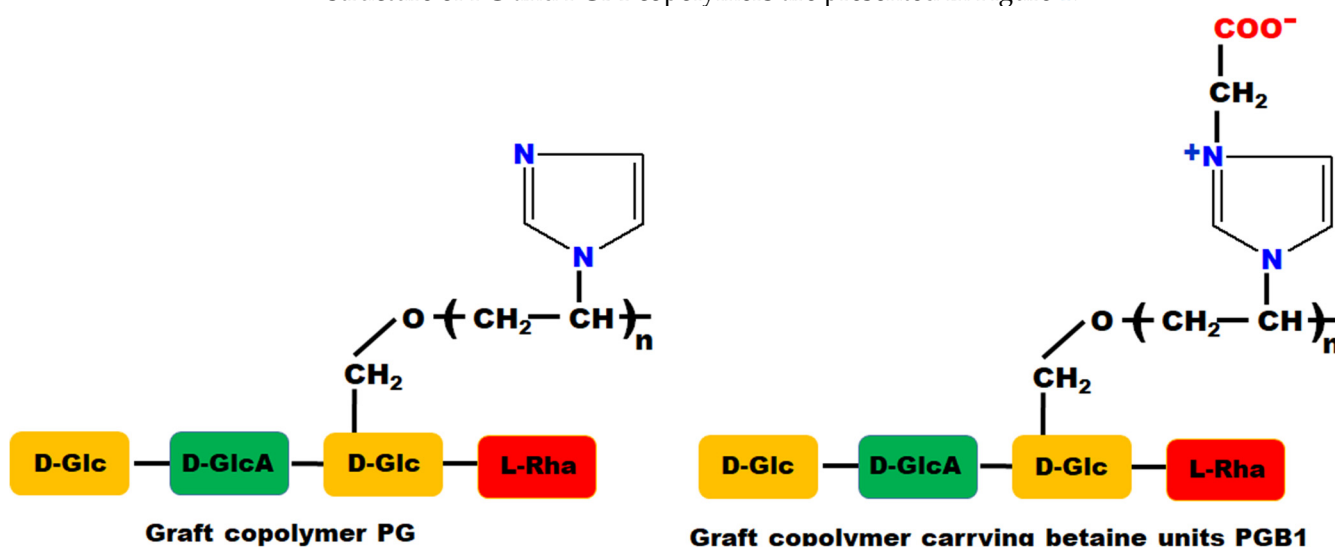
Figure 1. Chemical structure of PG and PGB1 graft porous copolymers.

In this paper, our investigations were directed to the following directions:
- Synthesis of new bioactive compounds in which thiadiazole and triazole structures are grafted onto the aromatic heterocycle, 2-mercaptobenzoxazole, followed by the choice of the compound with the best biological properties in order to be immobilized on a polymeric support;
- Synthesis of new polymer-bioactive compound systems; and
- Detailed studies on the immobilization of the bioactive compound by adsorption on grafted copolymers and those containing the betaine structure.

2. Results and Discussion

2.1. Synthesis of Thiadiazole and Triazole Derivatives

Among the heterocyclic combinations, the 1,3,4-thiadiazole and 1,2,4-triazole derivatives present a remarkable application interest. The synthesis of 1,3,4-thiadiazole and 1,2,4-triazole derivatives were performed in several steps as follows:

Step 1. Synthesis of 1-(benzoxazole-2′-yl-mercapto-acetyl)-4-aryl-thiosemicarbazides (II–VII) was performed in methanol solution by heating a mixture of benzoxazolyl-2-mercapto-acetic acid hydrazide (I) [43] with various types of isothiocyanate derivatives: phenyl, p-tolyl, p-methoxyphenyl, p-bromophenyl, p-chlorophenyl, and p-iodofenil, according to the procedures described in our previous papers for other types of thiosemicarbazides (Figure 2) [4,44,45].
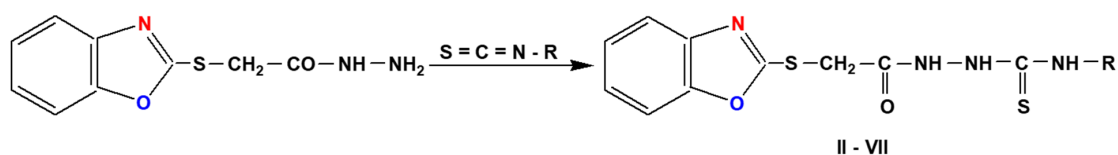
II, R = - C_6H_5; III, R = - C_6H_4 – CH_3 (p); IV, R = - C_6H_4 – OCH_3 (p); V, R = - C_6H_4 – Br (p); VI, R = - C_6H_4 – Cl (p); VII, R = - C_6H_4 – I (p).

Figure 2. Synthesis of 1-(benzoxazole-2′-yl-mercapto-acetyl)-4-aryl-thiosemicarbazides (II-VII).

The structure elucidation of the compounds II–VII was carried out by elemental analysis as well as by spectroscopic methods (FT-IR and ^{1}H-NMR).

The results obtained from the elemental analysis as well as the chemical formula and the yield of reaction of all bioactive compounds synthesized in this paper (compounds II-XIX) are presented in Table 1.

Table 1. Some characteristics of compounds II–XIX.

Samples	Elemental Analysis, Calc (Found) (%)								Chemical Formula	Yield (%)
	C	H	N	S	O	Br	Cl	I		
1,4-disubstituted thiosemicarbazides (compounds II–VII)										
II	53.6 (53.9)	3.9 (4.2)	15.6 (16)	17.9 (18.2)	8.9 (7.7)	-	-	-	$C_{16}H_{14}N_4O_2S_2$	65
III	54.8 (55.1)	4.3 (4.5)	15.1 (15.4)	17.2 (17.6)	8.6 (7.4)	-	-	-	$C_{17}H_{16}N_4O_2S_2$	75
IV	52.6 (52.9)	4.1 (4.3)	14.4 (14.8)	16.4 (16,9)	12.5 (11.1)	-	-	-	$C_{17}H_{16}N_4O_3S_2$	85
V	43.9 (44.1)	2.9 (3.2)	12.8 (12.9)	14.6 (15)	7.4 (6.3)	18.3 (18.6)	-	-	$C_{16}H_{13}N_4O_2S_2Br$	80
VI	48.9 (49)	3.3 (3.6)	14.3 (14.6)	16.3 (16.6)	8.2 (6.8)	-	9 (9.5)	-	$C_{16}H_{13}N_4O_2S_2Cl$	78
VII	39.7 (39.9)	2.7 (2.9)	11.6 (11.9)	13.2 (13.6)	6.6 (5.2)	-	-	26.2 (26.6)	$C_{16}H_{13}N_4O_2S_2I$	77
1,3,4-thiadiazoles (compounds VIII–XIII)										
VIII	56.5 (56.6)	3.5 (3.8)	16.5 (16.8)	18.8 (19.2)	4.7 (3.6)	-	-	-	$C_{16}H_{12}N_4OS_2$	89
IX	57.6 (58)	4 (4.1)	15.8 (16.1)	18.1 (18.5)	4.5 (3.3)	-	-	-	$C_{17}H_{14}N_4OS_2$	83
X	52.1 (52.4)	3.8 (4)	15.1 (15.4)	17.3 (17.6)	11.7 (10.6)	-	-	-	$C_{17}H_{14}N_4O_2S_2$	81
XI	45.8 (46.2)	2.6 (2.8)	13.4 (13.6)	15.3 (15.7)	22.9 (21.7)	19 (19.4)	-	-	$C_{16}H_{11}N_4OS_2Br$	79
XII	51.3 (51.4)	2.9 (3.1)	15 (15.3)	17.1 (17.4)	13.7 (12.8)	-	9.5 (9.7)	-	$C_{16}H_{11}N_4OS_2Cl$	74
XIII	41.2 (41.5)	2.4 (2.6)	12 (12.3)	13.7 (14.1)	30.7 (29.2)	-	-	27.3 (27.5)	$C_{16}H_{11}N_4OS_2I$	71

Table 1. *Cont.*

Samples	Elemental Analysis, Calc (Found) (%)								Chemical Formula	Yield (%)
	C	H	N	S	O	Br	Cl	I		
1,2,4-triazoles (compounds XIV–XIX)										
XIV	56.5 (56.7)	3.5 (3.9)	16.5 (16.9)	18.8 (19.2)	4.7 (3.3)	-	-	-	$C_{16}H_{12}N_4OS_2$	66
XV	57.6 (57.8)	4 (4.3)	15.8 (16.2)	18.1 (18.3)	4.5 (3.4)	-	-	-	$C_{17}H_{14}N_4OS_2$	74
XVI	55.1 (55.3)	3.8 (4)	15.1 (15.5)	17.3 (17.7)	8.7 (7.5)	-	-	-	$C_{17}H_{14}N_4O_2S_2$	88
XVII	45.8 (46)	2.6 (3)	13.4 (13.7)	15.3 (15.7)	22.9 (21.6)	19 (19.3)	-	-	$C_{16}H_{11}N_4OS_2Br$	79
XVIII	51.3 (51.4)	2.9 (3.3)	15 (15.2)	17.1 (17.4)	13.7 (12.7)	-	9.5 (9.9)	-	$C_{16}H_{11}N_4OS_2Cl$	77
XIX	41.2 (41.4)	2.4 (2.5)	12 (12.4)	13.7 (14)	30.7 (29.7)	-	-	27.3 (27.6)	$C_{16}H_{11}N_4OS_2I$	74

In the FT-IR spectra (Figure not shown), the following characteristic absorption bands can be observed: 700–749 cm^{-1} assigned to the C-S stretching vibration; 1400–1498 cm^{-1} attributed to the CH_2 bending vibration; 1620–1704 cm^{-1} assigned to the C=O stretching vibrations; the C=S stretching vibration was observed at 1120–1150 cm^{-1}; NH stretching vibration appears at 2880–3150 cm^{-1}; the absorption bands of the mono and disubstituted aromatic rings were identified in the region of 680–789 cm^{-1}; and the C-Br, C-Cl, and C-I stretching vibrations appear at 629 cm^{-1}, 725 cm^{-1}, and 630 cm^{-1}, respectively.

In the ^{1}H-NMR spectra, the two methylene protons generate a singlet at δ = 4.25–4.60 ppm and at δ = 8.67–8.89 ppm, while the protons from the -NH group appear at 10.06–10.85 ppm. The aromatic protons in phenyl and benzoxazole appear within the range 6.50–7.92 ppm. The protons belonging to the methyl groups are identified at δ = 2.11 ppm for the compound III and at δ = 3.38 ppm for the thiosemicarbazide IV (Figure 3).

Step 2. Synthesis of new 1,3,4-thiadiazoles and 1,2,4-triazoles starting from 1,4-disubstituted-thiosemicarbazides (compounds II–VII). The 5-aryl-amino-2-substituted-1,3,4-thiadiazoles (compounds VIII–XIII) were obtained by intramolecular cyclization in concentrated sulfuric acid medium, while the 5-mercapto-3,4-disubstituted -1,2,4-triazoles (compounds XIV–XIX) were prepared under the catalytic action of hydroxyl ions, according to our previously work described in literature (Figure 4) [4,44–47].

The idea of synthesis of grafted 1,3,4-thiadiazoles on the 2-mercapto-benzoxazole molecule is an extremely interesting possibility to find new derivatives, which can be active against some microbial strains.

The mechanism of the synthesis reaction of these types of heterocyclic compounds is presented in Figure 5 and contains the following steps:

In case of 1,2,4-triazoles, the mechanism of cyclization in the presence of hydroxyl ions (Figure 6) begins with the hydrogen extraction from the nitrogen atom situated at position 4 of 1,4-disubstituted thiosemicarbazide, which has an increased mobility due to the p-π conjugation between the lone pair electrons belonging to the nitrogen atom and the π electrons of thionic bond or of benzene nucleus, respectively. As a result of this conjugation, a negative charge appears on the nitrogen atom from position 4 that can be in equilibrium with another anion formed at the sulfur atom. In this mesomer ion, the negatively charged nitrogen atom (more stable) attacks the carbon belonging to the carbonyl group simultaneously with π electron delocalization, leading to the formation of the five-membered heterocycle, the negative charge being located at the oxygen atom outside the ring. This structure is stabilized by eliminating the hydroxyl group in the reaction medium leading to the formation of 5-mercapto-1,2,4-triazole structure. Depending on the preparation conditions and the reactant nature, as well as due to the presence of thioamide group in triazole molecule, 5-mercapto-3,4 disubstituted-1,2,4-triazoles show

the phenomenon of double reactivity, reacting as if they had a thionic structure (A) or a thiol structure (B). This behavior explains the presence of a reaction center at the sulfur atom from 5-position of five-membered heterocycle [48].
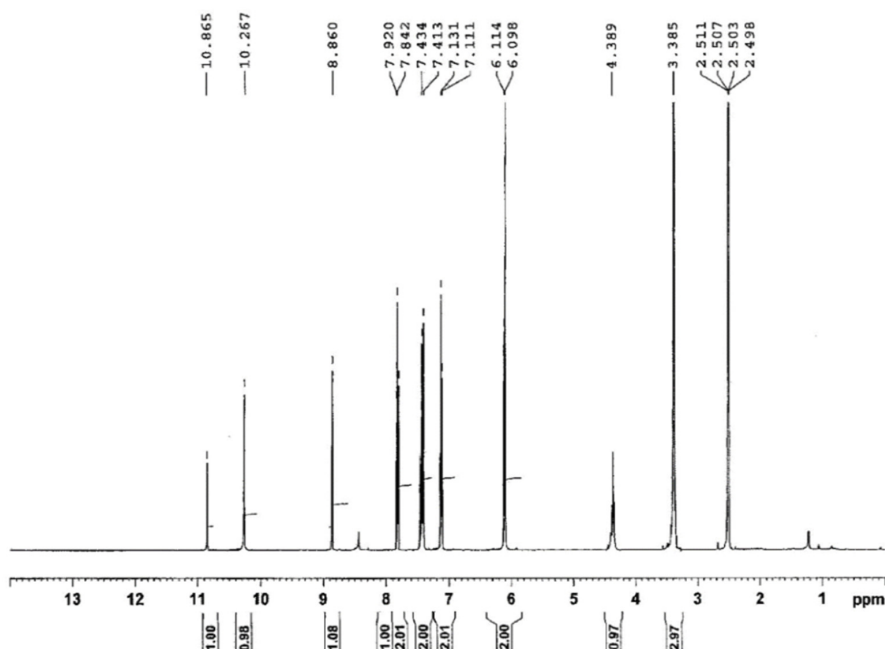
Figure 3. ^{1}H-NMR spectra of 1-(benzoxazole-2′-yl-mercapto-acetyl)-4-(p-methoxyphenyl)-thiosemicarbazide (compound IV).

5-aryl-amino-2-substituted-1,3,4-thiadiazoles   **5-mercapto-3,4-disubstituted-1,2,4-triazoles**

II, VIII, XIV, R = - C$_6$H$_5$; III, IX, XV, R = - C$_6$H$_4$ – CH$_3$ (p); IV, X, XVI, R = - C$_6$H$_4$ – OCH$_3$ (p); V, XI, XVII, R = - C$_6$H$_4$ – Br (p); VI, XII, XVIII, R = - C$_6$H$_4$ – Cl (p); VII, XIII, XIX, R = - C$_6$H$_4$ – I (p).
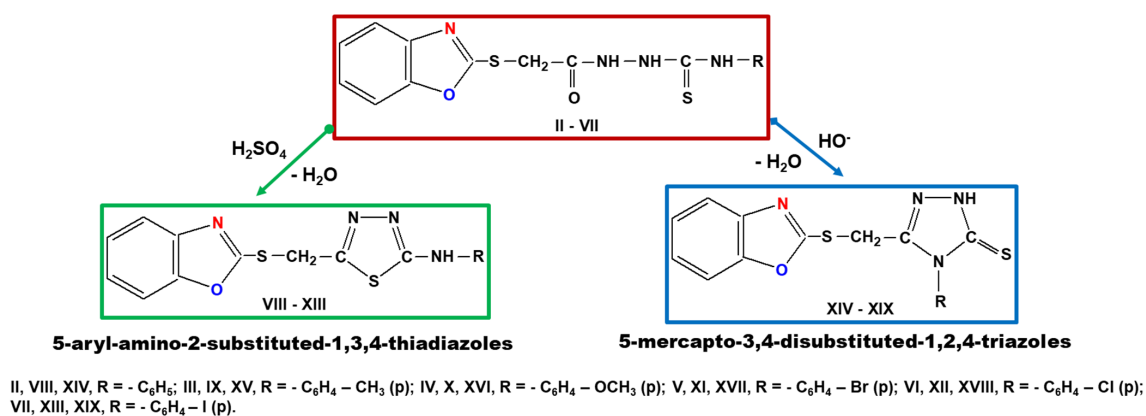
Figure 4. Synthesis of 1,3,4-thiadiazoles (compounds VIII–XIII) and 1,2,4-triazoles (compounds XIV–XIX).

VIII, R = - C$_6$H$_5$; IX, R = - C$_6$H$_4$ – CH$_3$ (p); X, R = - C$_6$H$_4$ – OCH$_3$ (p); XI, R = - C$_6$H$_4$ – Br (p); XII, R = - C$_6$H$_4$ – Cl (p); XIII, R = - C$_6$H$_4$ – I (p)

Figure 5. Intramolecular cyclization mechanism of reaction synthesis of 5-aryl-amino-2-substituted-1,3,4-thiadiazoles.

Figure 6. Cyclization mechanism of reaction synthesis of 5-mercapto-3,4-disubstituted-1,2,4-triazoles.

In order to obtain the information about the structure of 1,3,4-thiadiazoles (compounds VIII–XIII) and 1,2,4-triazoles (compounds XIV–XIX), the elemental analysis (Table 1) as well as the FT-IR (Figure 7) and ^{1}H-NMR spectra (Figure 8) were performed.

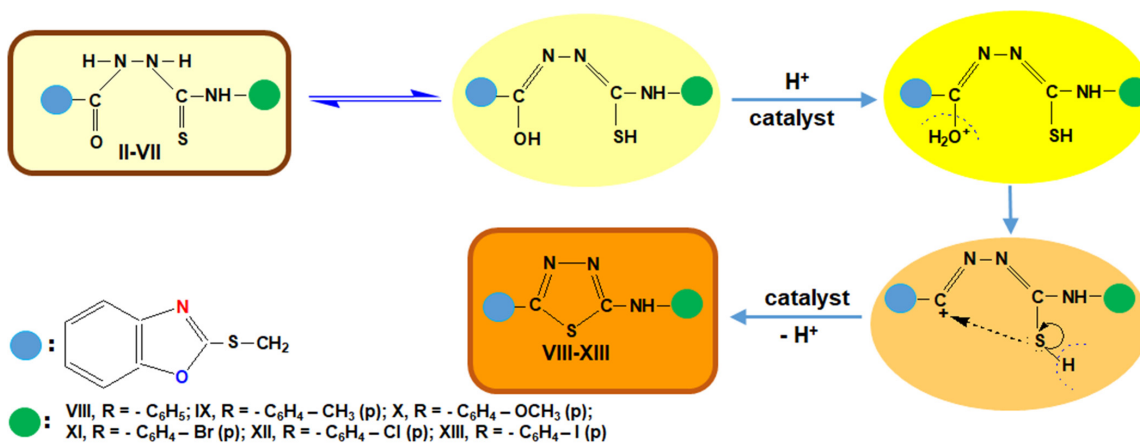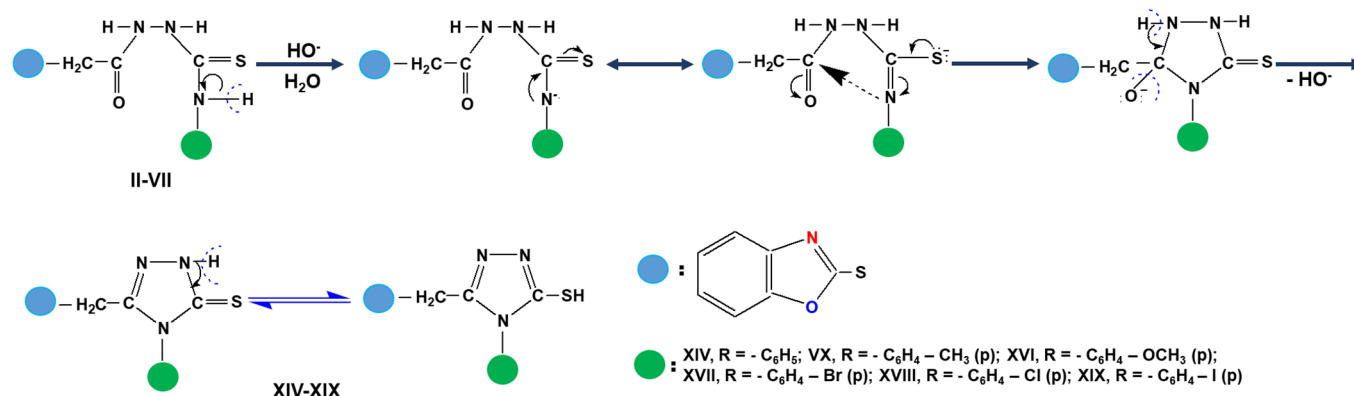Generally, in FT-IR spectra of the 1,3,4-thiadiazole (compounds VIII–XIII), the following absorption bands can be observed: the absorption bands at 3318–2880 cm^{-1} corresponding to the NH stretching vibrations; the absorption band at 1438–1462 cm^{-1} can be attributed to the stretching vibration of -N=C-S group; the bending vibration of the CH$_2$ group has been assigned to the absorption bands situated between 1401–1496 cm^{-1}; characteristic CH bands from mono and disubstituted benzene nucleus are assigned to the absorption band situated in the range of 680–789 cm^{-1}; and the C-Br, C-Cl, and C-I stretching vibrations appear at 629, 725, and 630 cm^{-1}, respectively.

In the case of 1,2,4-triazole derivatives, the FT-IR spectra of the compounds XIV–XIX present a wide band at 3553 cm^{-1} due to the NH stretching vibrations; 1613–1628 cm^{-1} corresponding to the C=N stretching vibration; the C=S group appears at 1490–1495 cm^{-1} while the bands at 837–942 cm^{-1} can be attributed to the para-disubstituted benzene nucleus; the S-CH$_2$ stretching vibration has been assigned to an adsorption band at 765–785 cm^{-1}; and the C-Br, C-Cl, and C-I stretching vibrations show maximum adsorption bands at 753, 746, and 748 cm^{-1}, respectively.

For example, in Figure 7, the spectra of compound VIII (a) and compound XVI (b), respectively, are presented.

^{1}H-NMR spectra bring additional arguments regarding the structure of the obtained organic compounds. In case of 1,3,4-thiadiazole derivatives, the protons of the CH$_2$ group bound to the sulfur atom situated at position 2′ of the benzoxazole nucleus appear as a singlet in the region of 4.25–4.53 ppm. The proton bound to the nitrogen could be detected as a singlet in the region 10.27–10.98 ppm. For all types of 1,3,4-thiadiazoles, aromatic protons appear at 6.91–7.56 ppm and 8.21–8.57 ppm, respectively. The protons of the methyl group in 1,3,4-thiadiazoles (compounds IX and X) are found as a triplet at 2.98 and 3.38 ppm, respectively.

The ^{1}H-NMR spectra of 1,3,4-thiadiazoles (compound VIII) and 1,2,4-triazoles (compound XVI) are presented in Figure 8.

The ^{1}H-NMR spectra of the 1,2,4-triazole derivatives (compounds XIV–XIX) present a singlet due to the protons of the CH$_2$ group at 4.17–4.18 ppm, while at 14.04–14.33 ppm is observed a singlet specific to the proton belonging to the NH group. For all 1,2,4-triazoles, the aromatic protons appear at 6.99–7.85 ppm, and for compounds XV and XVI, the protons of the methyl group appear at 2.43 and 3.43 ppm, respectively.
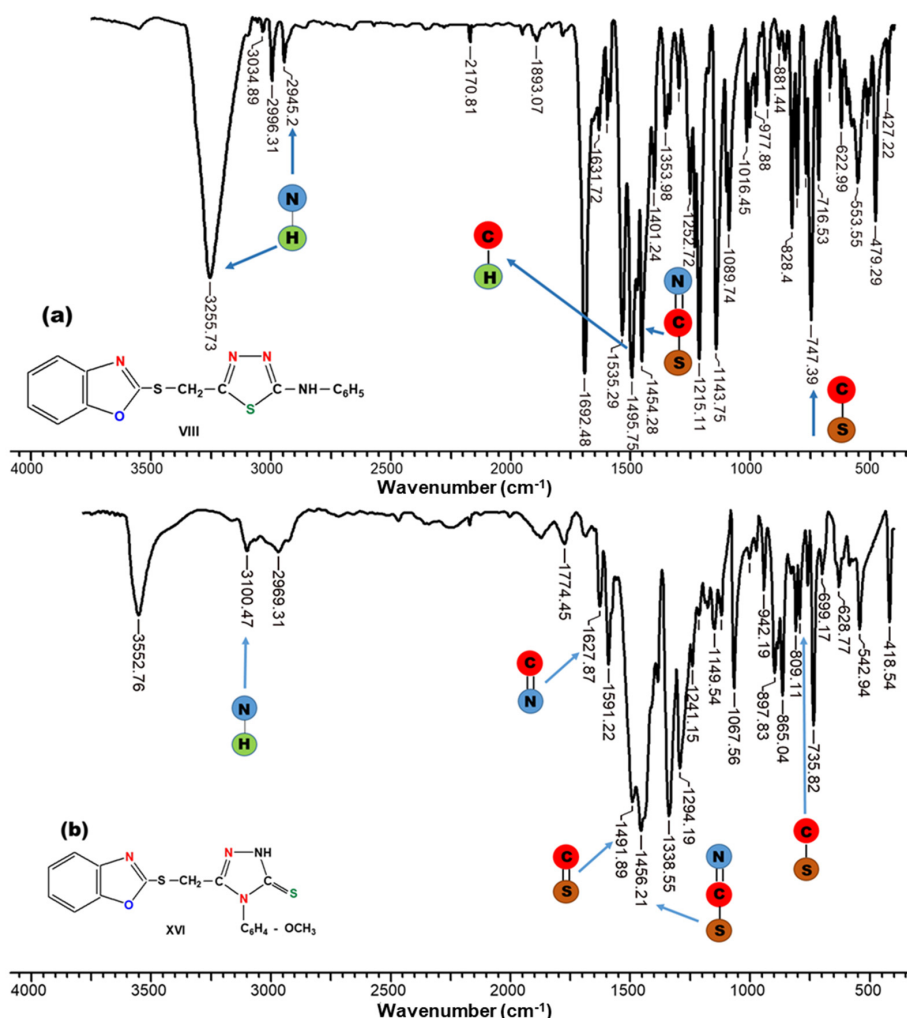
Figure 7. FT-IR spectrum of (**a**) 1,3,4-thiadiazoles (compound VIII) and (**b**) 1,2,4-triazole (compound XVI).
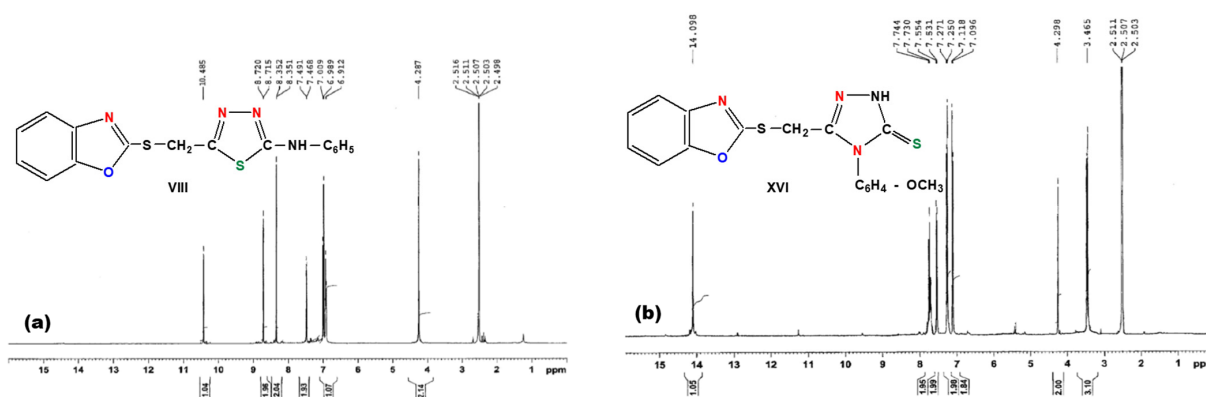
Figure 8. ^{1}H-NMR spectra of (**a**) 1,3,4-thiadiazoles (compound VIII) and (**b**) 1,2,4-triazoles (compound XVI).

2.2. Antibacterial Activities of Bioactive Compounds

The antimicrobial activity of 1,3,4 thiadiazoles and 1,2,4 triazoles was tested according to the National Committee for Clinical Laboratory Standards Institute NCCLS Approval Standard Document M2-A5, Vilanova, PA, USA (2000), on the following microbial strains: gram-positive bacteria (*Staphylococcus aureus* (ATCC-2593), *Bacillus subtilis* (ATCC-6638), *Bacillus cereus* (ATCC-10876)) and gram-negative bacteria (*Salmonella enteritidis* (P-1131) and *Escherichia coli* (ATCC-25922)).

The results regarding the antimicrobial activity of the bioactive compounds synthesized can be seen in Table 2.

Table 2. Antibacterial spectra of 1,3,4-thiadiazoles and 1,2,4- triazoles.

Sample Code	Time for Thermostating (h)	Staphylococcus aureus mg/mL			Bacillus subtilis mg/mL			Bacillus cereus mg/mL			Salmonella enteritidis mg/mL			Escherichia coli mg/mL		
		1	0.5	0.25	1	0.5	0.25	1	0.5	0.25	1	0.5	0.25	1	0.5	0.25
VIII	24	-	+	●	-	-	●	+	+	+	+	+	+	-	-	●
	48	-	-	-	-	-	●	-	+	+	+	+	+	-	●	●
IX	24	●	●	-	●	●	+	+	+	+	+	+	+	-	●	●
	48	●	●	-	●	●	+	+	+	+	+	+	+	●	●	●
X	24	●	●	●	●	●	-	+	-	-	+	+	+	-	-	●
	48	●	●	●	●	+	-	+	+	+	+	+	-	●	●	●
XI	24	+	●	●	●	●	●	+	+	+	+	+	+	●	●	●
	48	+	●	+	●	●	+	+	+	+	+	+	+	●	●	●
XII	24	●	●	●	●	●	+	+	+	+	+	+	+	●	●	●
	48	●	+	●	●	●	+	+	+	+	+	+	+	●	●	●
XIII	24	●	+	●	●	●	+	+	+	+	+	+	+	●	●	●
	48	●	+	●	●	●	+	+	+	+	+	+	+	●	●	●
XIV	24	-	●	●	-	-	-	-	●	●	-	-	-	-	-	-
	48	●	+	+	●	+	+	+	+	+	-	-	-	-	-	-
XV	24	-	-	-	-	-	-	●	●	●	-	-	-	-	-	-
	48	-	●	-	-	-	-	+	+	+	-	-	-	-	-	-
XVI	24	-	-	-	-	-	-	●	●	●	-	-	-	-	-	-
	48	-	-	-	-	-	-	+	+	+	-	-	-	-	-	-
XVII	24	●	●	●	●	●	●	●	●	●	●	●	●	●	●	●
	48	+	+	+	+	+	+	+	+	+	+	+	+	+	+	+
XVIII	24	●	●	●	●	●	●	●	●	●	●	●	●	●	●	●
	48	+	+	+	+	+	+	+	+	+	+	+	+	+	+	+
XIX	24	●	●	●	●	●	●	●	●	●	●	●	●	-	●	●
	48	+	+	+	+	+	+	+	+	+	+	+	+	+	+	+
Kanamycine	24	-	-	-	-	-	-	-	-	-	-	-	+	-	-	-
	48	-	-	-	-	-	-	-	●	-	-	-	+	-	-	+

- no growth; ● moderate growth; + normal growth.

Experimental data shows that 1,3,4-thiadiazoles (compounds VIII–XIII) are sensitive to *Staphyloccocus aureus* and present a moderate effect on *Bacillus subtilis* and *Escherichia coli*, while the culture of *Bacillus cereus* and *Salmonella enteritidis* are resistant to the action of the 1,3,4-thiadiazole test.

The 1,2,4-triazoles (compounds XIV–XVI) have been shown to be strong inhibitors on the growth of the bacteria *Escherichia coli*, *Salmonella enteritidis*, and *Bacillus subtilis* in any concentration and regardless of the contact time, while against *Staphylococcus aureus* and *Bacillus cereus* germs, the 1,2,4-triazoles show a moderate action. In contrast, the 1,2,4-triazoles (compounds XVII–XIX) show a moderate action on all tested germs only in a short period of contact time and at all concentrations. It can be stated that the tested 1,3,4-thiadiazoles and 1,2,4-triazoles show appreciable antimicrobial activity against microbial strains similar to that of the model drug, kanamycin.

2.3. Immobilization Studies of Triazoles

Among the new synthesized compounds, the 1,2,4-triazole derivative obtained with the highest yield (88%) and the best antimicrobial activity, namely 3-(benzoxazole-2′-yl-mercapto-methyl)-4-(p-methoxyphenyl)-5-mercapto-1,2,4-triazole (compound XVI), which was selected for immobilization by sorption onto grafted copolymers.

The interaction between PG and PGB1 copolymers and compound XVI was highlighted by FT-IR spectroscopy (Figure 9).
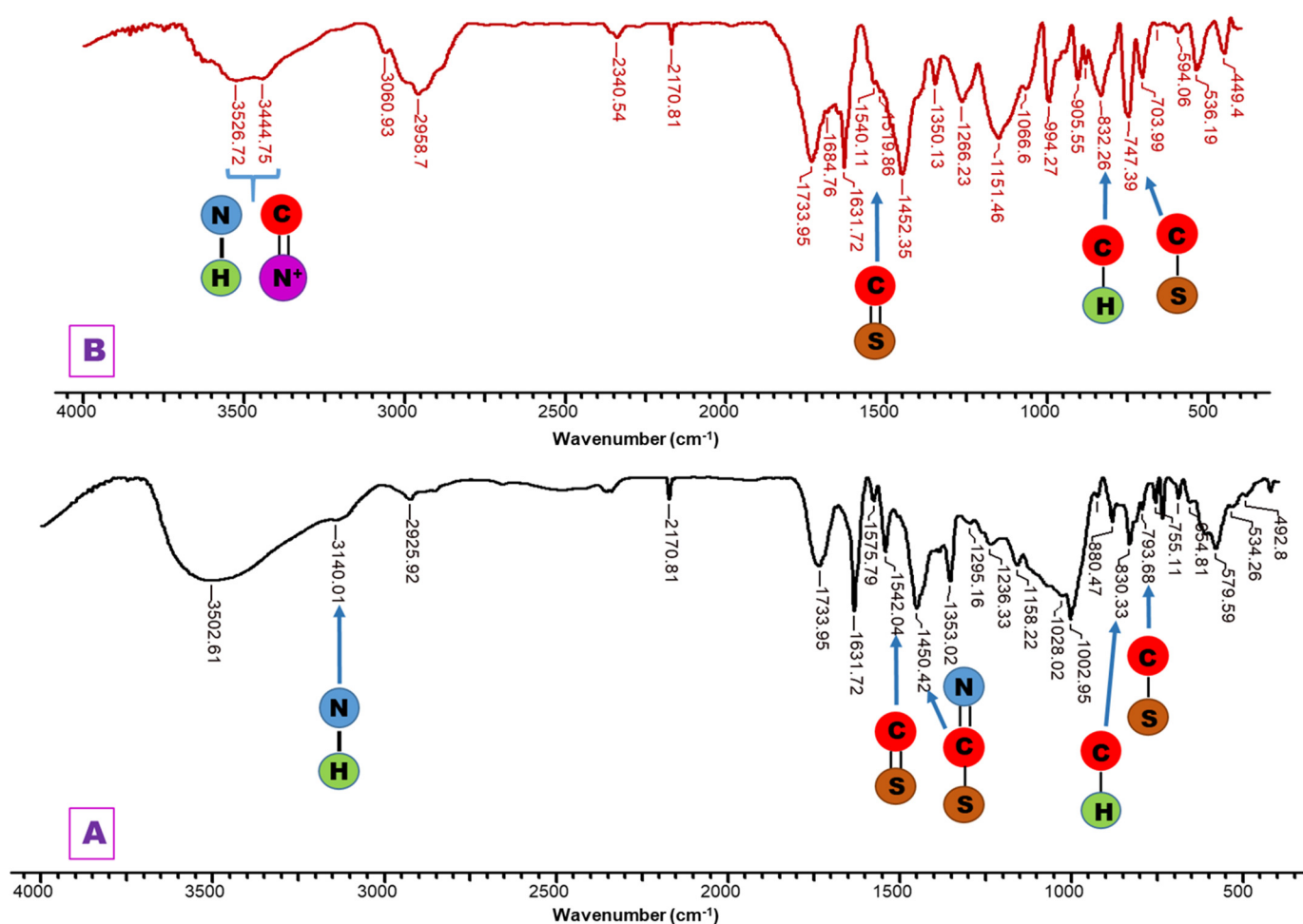
Figure 9. FT-IR spectra for (**A**) PG-T system; (**B**) PGB1-T system.

- For PG—1,2,4-triazole systems (PG-T), it can be observed some new absorption bands as follows: the absorption band at 3140 cm^{-1} due to the stretching vibration of -NH group; 1542 cm^{-1} assigned to the stretching vibration of C=S group; 1450 cm^{-1} corresponding to the stretching vibration of -N=C-S group; and 793 cm^{-1} assigned to the stretching vibration of S-CH$_2$ group.
- For PGB1—1,2,4-triazole systems (PGB1-T), the changes that occur in the FTIR spectrum are the following: the band vibration of 3439 cm^{-1} from PGB1 copolymer is shifted in PGB1-T spectra to 3445 cm^{-1} due to the overlap of the absorption band of -C=N$^+$ group from PGB1 copolymer, with absorption band corresponding to the -NH group belonging to the 1,2,4-triazole; absorption band at 832 cm^{-1} is assigned to the stretching vibration of C-H out of plane bending.

Also, XRD and SEM studies were performed for a better characterization of PG-T and PGB1-T systems. The XRD patterns of 1,2,4-triazole, PG-T, and PGB1-T are presented in Figure 10.

The XRD analysis of PG-T and PGB1-T systems showed the combined signals of both PG/PGB1 copolymers and 1,2,4-triazole, leading to the conclusion that the 1,2,4-triazole was successfully immobilized onto polymeric supports.

Visualization of surface morphology of PG-T and PGB1-T systems was achieved through SEM microscopy with a magnification of 1000, and the images are presented in Figure 11.
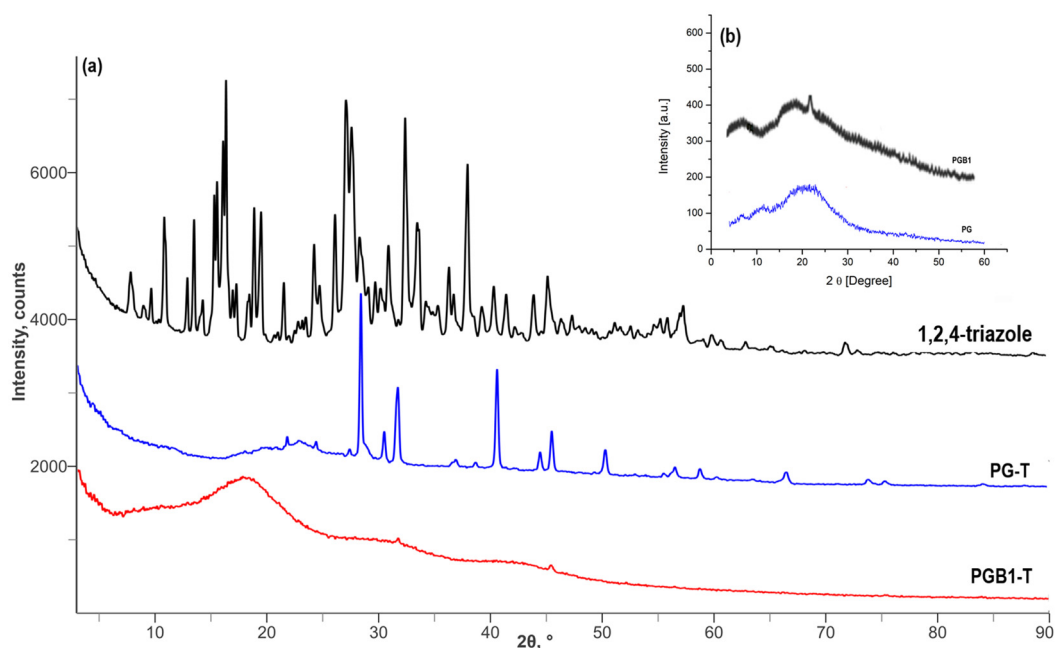
Figure 10. XRD patterns of 1,2,4-triazole, PG-T, and PGB1-T systems (**a**) and of PG and PGB1 copolymers (**b**).
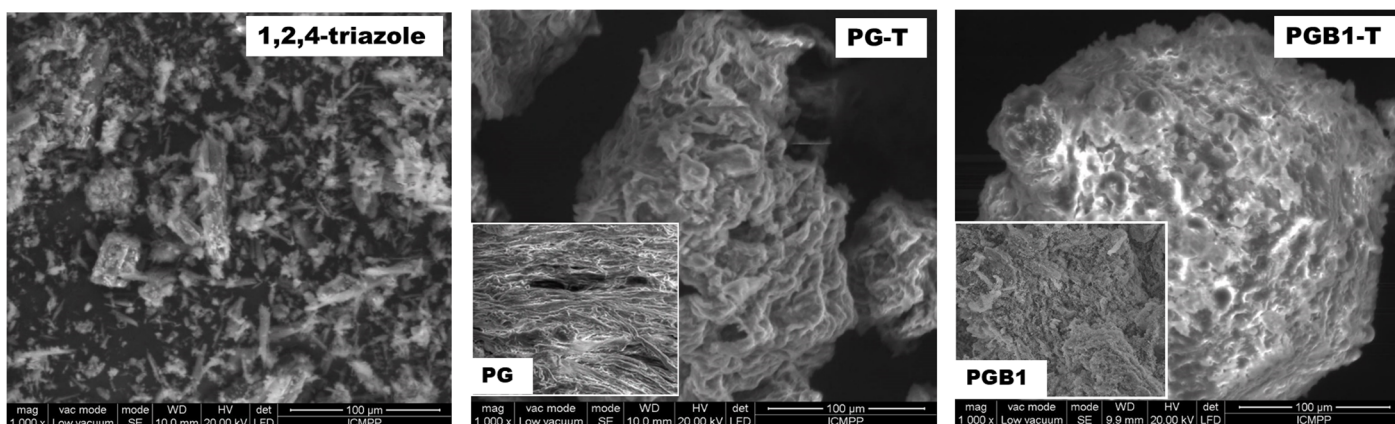

Figure 11. SEM images for 1,2,4-triazole, PG-T, and PGB1-T systems.

From SEM images, it can be observed that the PG-T and PGB1-T systems appear to have porous structures different from those of PG and PGB1 copolymers. The changes in the surface morphologies of PG-T and PGB1-T systems indicate that the sorption of 1,2,4-triazole onto polymeric support occurred.

Generally, in order to evaluate a sorption process of bioactive compound, it is important to consider two physico-chemical aspects, namely the equilibrium and the kinetics of sorption.

2.3.1. Sorption Isotherms

To describe the interactions between sorbate and sorbent that occurs in sorption processes, three model isotherms were used, namely: Langmuir, Freundlich, and Dubinin–Radushkevich.

- Langmuir isotherm

The Langmuir isotherm describes the sorption in a homogeneous system [49] and is given by the equation:

$$q_e = \frac{q_m \cdot K_L \cdot C_e}{1 + K_L \cdot C_e} \tag{1}$$

where: q_e represents the amount of 1,2,4-triazole sorbed at equilibrium (mg/g); q_m represents the maximum amount sorbed (mg/g); C_e is the concentration of 1,2,4-triazole solution at equilibrium (mg/L); and K_L is the Langmuir constant that reflects the affinity between sorbate and sorbent.

To determine whether the sorption system used is favorable or unfavorable to the sorption, the equilibrium parameter R_L, given by the equation [50], was also calculated:

$$R_L = \frac{1}{1 + K_L.C_i} \tag{2}$$

where C_i represents the initial concentration. According to the literature [51], if $R_L < 1$, then the sorption is unfavorable, for $R_L = 1$, the sorption is linear; if $0 < R_L < 1$, the sorption is favorable or irreversible if $R_L = 0$.

- Freundlich isotherm

Another model used in sorption studies is the Freudlich isotherm. This isotherm model is applied in the case of multilayer sorption of sorbate on a heterogeneous surface [52]. The Freundlich isotherm is described by the following equation:

$$q_e = K_F \cdot C_e^{1/n_f} \tag{3}$$

where K_F is the Freundlich constant which represents the amount of 1,2,4-triazole sorbed per gram of sorbent when the equilibrium concentration is equal to unity (L/g); $1/n_f$ indicates the type of isotherm as follows: favorable $0 < 1/n_f < 1$ or unfavorable $1/n_f > 1$.

- Dubinin–Radushkevich isotherm

The Dubinin–Radushkevich isotherm is an empirical model designed to estimate the apparent free energy of sorption as well as to differentiate between the physical and chemical sorption process [53]. The Dubinin–Radushkevich model equation is given by the following mathematical relation:

$$q_e = q_{DR} \cdot exp\left\{ -\beta \left[RTln\left(1 + \frac{1}{C_e} \right) \right]^2 \right\} \tag{4}$$

where q_{DR} represents the maximum amount sorbed (mg/g); β is the Dubinin–Radushkevich constant (mol²/kJ²); R represents the ideal gas constant (R = 8.314 kJ/mol·K); and T is the temperature (K).

The Dubinin–Radushkevich isotherm constant, β, is associated with the average free sorption energy, E (kJ/mol), calculated using the following equation:

$$E = 1(2\beta)^{\frac{1}{2}} \tag{5}$$

The value of E is used to obtain information about the nature of the sorption process. The sorption process can be physical when the E values are between 1 and 8 kJ/mol, ion exchange for values of E between 8 and 16 kJ/mol, and chemical nature for values of E greater that 16 kJ/mol [54].

The parameters of the studied isotherms as well as the values of the error functions R^2 and χ^2 are presented in Table 3.

Table 3. Parameter values corresponding to Langmuir, Freundlich, and Dubinin–Radushkevich isotherms calculated in case of 1,2,4-triazole sorption on PG and PGB1 copolymers at different temperatures.

	PG			PGB1		
	298	**303**	**308**	**298**	**303**	**308**
Langmuir model						
q_m (mg/g)	478	533	636	537	616	685
K_L (L/mg)	0.068	0.086	0.109	0.098	0.126	0.161
R_L	0.01–0.29	0.01–0.25	0.10–0.20	0.01–0.22	0.01–0.18	0.004–0.15
χ^2	3.324	2.613	3.429	2.700	2.010	2.150
R^2	0.994	0.993	0.997	0.993	0.992	0.996
Freundlich model						
K_F (L/g)	0.457	0.512	0.617	0.528	0.602	0.673
$1/n_f$	0.939	0.738	0.729	0.686	0.540	0.383
χ^2	33.462	23.958	38.332	25.213	19.219	18.782
R^2	0.911	0.920	0.915	0.913	0.921	0.914
Dubinin–Radushkevich model						
q_{DR} (mg/g)	463	521	629	532	612	679
E (kJ/mol)	1.099	1.561	2.171	1.357	2.608	3.714
χ^2	0.402	0.359	0.413	0.371	0.226	0.277
R^2	0.998	0.997	0.998	0.998	0.999	0.998

From data presented in Table 3, the following conclusions can be drawn:

- The theoretical values obtained for the maximum sorption capacity (q_m) calculated on the basis of the Langmuir isotherm are close to the experimental values q_c (457, 512 and 618 mg 1,2,4-triazole /g PG copolymer and 529, 601 and 672 mg of 1,2,4-triazole /g PGB1 copolymer);
- The values of the equilibrium parameter, R_L, were in the range between 0 and 1, thus confirming that the PG and PGB1 copolymers are favorable supports for the sorption of 1,2,4-triazoleat at the three temperatures studied. It is also observed that the K_L values are higher in the case of the PGB1 copolymer than in the case of the PG copolymer, which indicates a higher affinity of the PGB1 copolymer for 1,2,4-triazole; this is in agreement with the highest sorption capacity obtained in the case of the PGB1 copolymer;
- The values for R^2 and χ^2 are in the range of 0992–0.997 and 2.010–3.429, respectively, indicating that the Langmuir isotherm describes well the experimental data;
- Although the values of $1/n_f$ are in the range of 0–1, which indicates that the Freundlich isotherm is favorable in the case of 1,2,4-triazolesorption onto PG and PGB1 copolymers, the small values of R^2 (0.911 to 0.921) associated with high values of χ^2 (18.782–38.332) shows that the Freundlich isotherm does not describe well the experimental data;
- The analysis of the parameter values obtained by applying the Dubinin–Radushkevich isotherm shows that the q_{DR} values are very close to the experimental values, which indicates that this isotherm describes well the experimental data. This is also supported by the fact that high values for R^2 (0.997–0.999) and low values for χ^2 (0.226–0.413) were obtained, confirming that the Dubinin–Radushkevich isotherm describes very well the sorption of 1,2,4-triazole onto PG and PGB1 copolymers;
- The calculated values of the average free energy of 1,2,4-triazole sorption onto PG and PGB1 copolymers are in the range of 1.099–3.714 kJ/mol, which indicates that the sorption process studied is physical in nature.

2.3.2. Thermodynamic Parameters

By means of thermodynamic parameters, such as Gibbs free energy change (ΔG), enthalpy change (ΔH), and entropy change (ΔS), the mechanism and the type of sorption process can be determined. Thus, according to the literature [55], it is known that in the case

of physical sorption, the values of ΔH are less than 40 kJ/mol, while in the case of chemical sorption, the values of ΔH are in the range of 40–120 kJ/mol. The value of ΔH and ΔS can be determined by means of the Langmuir constant using the Van 't Hoff equation [56]:

$$ln K_L = \frac{\Delta S}{R} - \frac{\Delta H}{RT} \qquad (6)$$

From the linear representation ln K_L versus $1/T$ (Figure 12), the values of ΔS and ΔH were obtained from the intercept and slope, respectively, and the results are presented in Table 4. The values of ΔG were obtained using the following equation:

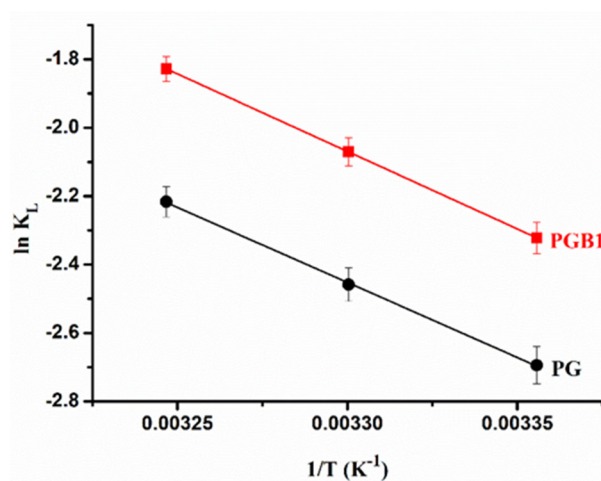$$\Delta G = \Delta H - T\Delta S \qquad (7)$$

Figure 12. Plots of lnK_L versus $1/T$ for sorption of 1,2,4-triazole derivative onto PG and PGB1 copolymers.

Table 4. Thermodynamic parameters of sorption process.

Sample Code	ΔH (kJ/mol)	ΔS (J/mol·K)	R^2	ΔG (kJ/mol)		
				298 K	303 K	308 K
PG	36.49	100.05	0.995	−29.78	−30.278	−30.78
PGB1	37.67	107.14	0.998	−31.89	−32.425	−32.96

As it can be seen from Table 4, the negative values of ΔG show that the 1,2,4-triazole sorption onto PG and PGB1 copolymers is spontaneous and favorable. Also, the values of this thermodynamic parameter decrease with increasing of the temperature, indicating that there is a higher efficiency of the sorption process at higher temperatures. The values of $\Delta H < 40$ kJ/mol indicate that the interactions between the PG or PGB1 copolymers and 1,2,4-triazole are physical in nature. On the other hand, the positive value of the ΔH shows that the sorption process is endothermic and the increase of the temperature leads to an increase in the amount of 1,2,4-triazole sorbed. The positive value of ΔS indicates the affinity of PG and PGB1 copolymers for 1,2,4-triazole as well as the increase randomness at the solid-solution interface during the sorption process [57]. Also, the positive value of ΔS can indicate an increase in the degree of freedom of 1,2,4-triazole. Moreover, the positive values of ΔH and ΔS lead to the conclusion that the sorption process occurs spontaneously at all temperatures.

2.3.3. Sorption Kinetic Study

The study of sorption kinetic describes the rate of sorption and is very important because it gives us information about the mechanism of sorption. Two mathematical models, such as the Lagergren model (pseudo-first order kinetic model) and the Ho model (pseudo-second order kinetic model), were used to elucidate the mechanism of 1,2,4-triazole

sorption onto PG and PGB1 copolymers. The two models mentioned above are described by the following equations:

- Lagergren model [58]:

$$q_t = q_e\left(1 - e^{-k_1 t}\right) \tag{8}$$

- Ho model [59]:

$$q_t = \frac{k_2 \cdot q_t^2 \cdot t}{1 + k_2 \cdot q_e \cdot t} \tag{9}$$

where q_e and q_t are the amounts of 1,2,4-triazole sorbed at equilibrium and at time t (mg/g), k_1 is the rate constant of the pseudo-first order sorption process (min^{-1}), and k_2 is the rate constant of pseudo-second order sorption process (g/mg·min).

Figure 13 presents the plots of the Lagergren and Ho models in the case of 1,2,4-triazole sorption ($C_{1,2,4\text{-triazole}} = 15 \times 10^{-3}$ g/mL) onto PG and PGB1 copolymers at $T = 308$ K, and Table 5 shows the parameter values corresponding to the Lagergren and Ho models.
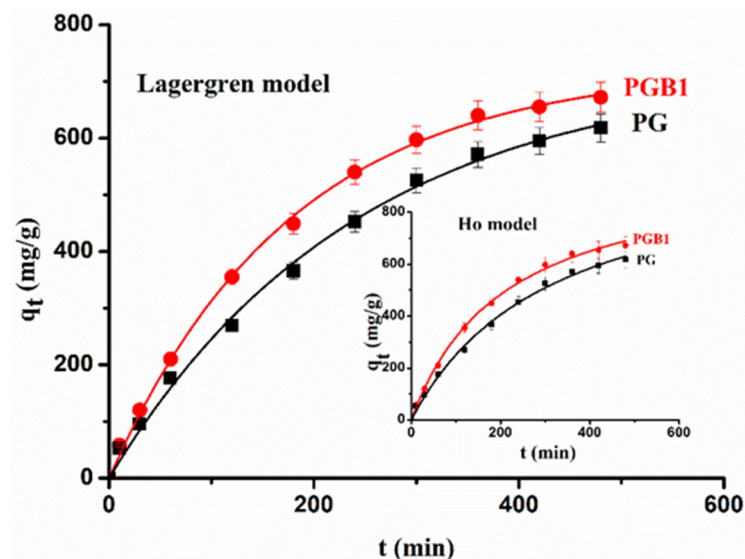

Figure 13. Graphical representation of Lagergren and Ho models in case of 1,2,4-triazole sorption onto PG and PGB1 copolymers at $T = 308$ K and $C_{1,2,4\text{-triazole}} = 15 \times 10^{-3}$ g/mL.

Table 5. The parameters corresponding to the Lagergren and Ho models used in the case of 1,2,4-triazole sorption onto PG and PGB1 copolymers.

$C_{1,2,4\text{-triazole}}$ (g/mL)		PG			PGB1		
		298	303	308	298	303	308
	$q_{e,exp}$ (mg/g)	325	394	473	412	496	587
				Lagergren model			
	$q_{e,calc}$ (mg/g)	346.29	415.91	491.95	428.82	511.76	600.94
	k_1 ($\times 10^3$ min^{-1})	2.19	3.01	3.31	3.83	3.92	4.14
	χ^2	1.738	2.263	1.119	1.119	1.682	1.103
	R^2	0.998	0.998	0.998	0.999	0.998	0.999
3.6×10^{-4}				Ho model			
	$q_{e,calc}$ (mg/g)	449.72	482.38	564.84	579.40	616.92	696.22
	k_2 [$\times 10^6$ (g/mg· min)]	1.26	1.62	2.43	2.89	3.51	3.92
	χ^2	4.014	4.686	5.976	2.411	5.499	5.040
	R^2	0.997	0.997	0.997	0.998	0.997	0.998

Table 5. *Cont.*

$C_{1,2,4-triazole}$ (g/mL)		PG			PGB1		
		298	**303**	**308**	**298**	**303**	**308**
	$q_{e,exp}$ (mg/g)	**325**	**394**	**473**	**412**	**496**	**587**
	$q_{e,exp}$ (mg/g)	432	491	593	507	583	659
				Lagergren model			
3.6 × 10⁻³	$q_{e,calc}$ (mg/g)	473.63	523.96	622.21	531.87	606.53	679.53
	k_1 (×10³ min⁻¹)	3.10	3.52	4.01	4.13	4.27	4.87
	χ^2	1.456	1.446	1.569	1.312	1.852	1.786
	R^2	0.998	0.999	0.998	0.997	0.998	0.997
				Ho model			
	$q_{e,calc}$ (mg/g)	546.70	621.17	709.71	649.28	694.28	766.03
	k_2 [×10⁶ (g/mg· min)]	2.19	2.46	3.11	3.07	3.72	4.01
	χ^2	2.071	2.539	2.390	2.772	2.083	2.310
	R^2	0.997	0.996	0.997	0.995	0.997	0.996
	$q_{e,exp}$ (mg/g)	449	504	606	519	594	667
				Lagergren model			
7 × 10⁻³	$q_{e,calc}$ (mg/g)	463.71	527.91	622.32	533.86	621.43	681.07
	k_1 (×10³ min⁻¹)	3.42	3.96	4.43	4.60	4.90	5.10
	χ^2	1.722	1.949	1.654	1.034	1.326	1.764
	R^2	0.997	0.997	0.998	0.998	0.997	0.999
				Ho model			
	$q_{e,calc}$ (mg/g)	567.15	613.04	713.83	621.28	734.63	796.60
	k_2 [×10⁶ (g/mg min)]	3.09	3.87	4.11	3.35	4.19	5.17
	χ^2	2.609	2.913	1.895	2.776	2.864	3.775
	R^2	0.996	0.997	0.996	0.997	0.997	0.998
	$q_{e,exp}$ (mg/g)	457	512	618	529	601	672
				Lagergren model			
15 × 10⁻³	$q_{e,calc}$ (mg/g)	483.63	532.96	644.21	544.25	627.05	694.28
	k_1 (×10³ min⁻¹)	3.67	4.67	4.81	4.92	5.14	5.48
	χ^2	1.466	1.343	1.691	1.144	1.671	1.024
	R^2	0.997	0.999	0.998	0.998	0.999	0.999
				Ho model			
	$q_{e,calc}$ (mg/g)	568.17	624.11	754.83	635.77	729.27	783.34
	k_2 [×10⁶ (g/mg min)]	3.85	4.38	5.83	4.23	4.97	5.73
	χ^2	3.050	3.208	3.903	3.887	4.321	3.678
	R^2	0.996	0.997	0.996	0.998	0.997	0.997

From data presented in Table 5, it is observed that the value of the sorption rate increases with the increase of the 1,2,4-triazole concentration. The highest amount of 1,2,4-triazole sorbed was obtained in the case of the PGB1 copolymer. The q_e values calculated by applying the Lagergren model are close to the experimental values compared to the q_e values calculated by applying the Ho model. Although the values of the correlation coefficients R^2 are higher when applying the two kinetic models, the χ^2 values are higher when applying the Ho model, which indicates that the Lagergren model describes better the experimental data. These results indicate that 1,2,4-triazole sorption onto PG and PGB1 copolymer is a physical process.

2.4. In Vitro Release Studies

In vitro release studies were performed on the PG-T and PGB1-T systems with the highest amount of immobilized 1,2,4-triazole. In vitro 1,2,4-triazole release studies were realized at pH = 1.2, and the release profiles are shown in Figure 14.
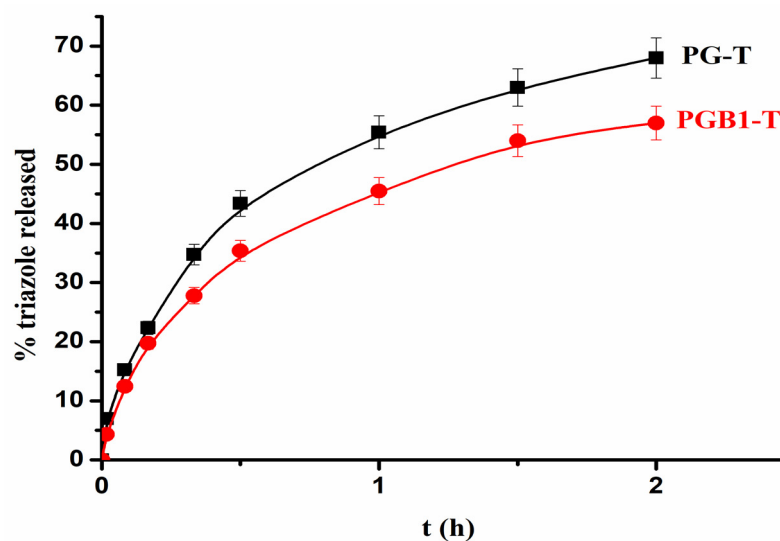
Figure 14. Release profiles of 1,2,4-triazole from PG-T and PGB1-T systems at pH = 1.2.

The kinetic studies and the release mechanism from PG-T and PGB1-T copolymers loaded with 1,2,4-triazole were examined using the following mathematical models:

- Higuchi model [60]:

$$Q_t = k_H \cdot t^{1/2} \tag{10}$$

where Q_t is the amount of drug released at time t; k_H is the Higuchi dissolution constant; and t is the time.

- Korsmeyer–Peppas model [61]:

$$\frac{M_t}{M_\infty} = k_r \cdot t^n \tag{11}$$

where M_t/M_∞ is the fraction of drug released at time t; k_r is the release rate constant that is characteristic to bioactive compound-polymer interactions; and n is the diffusion coefficient that is characteristic to the release mechanism. The values of the 1,2,4-triazole release parameters from PG-T and PGB1-T systems are presented in Table 6.

Table 6. Kinetic parameters of 1,2,4-triazole release from PG-T and PGB1-T systems.

Sample Code	Higuchi Model		Korsmeyer–Peppas Model		
	k_H (h$^{-1/2}$)	R^2	k_r (min^{-n})	n	R^2
PG-T	0.324	0.993	0.014	0.534	0.995
PGB1-T	0.294	0.994	0.017	0.634	0.996

The release exponent n from the Korsmeyer–Peppas equation is situated between 0.534 and 0.634. These results suggest that the release mechanism of 1,2,4-triazole from PG-T and PGB1-T systems was controlled by more than one process, namely diffusion and swelling.

3. Materials and Methods

3.1. General Information

All reactants and solvents were purchased from Merck Company KGaA (Darmstadt, Germany) and were used without purification. Elemental analyses were performed by Exeter Analytical CF-440 Elemental Analyzer (Coventry, United Kingdom). The bioactive compounds (1,4-disubstituted-thiosemicarbazides, 1,3,4-thiadiazoles, and 1,2,4-triazoles) were characterized by FT-IR spectroscopy (Bruker Vertex FT-IR spectrometer) as potassium

bromide pellets in the range of 4000–400 cm^{-1} and at a resolution of 2 cm^{-1}. The ^{1}H NMR spectra were recorded in DMSO-d$_{60}$ on Bruker ARX 400 Spectrometer (400 MHz). X-ray diffraction analysis was performed in a Rigaku Miniflex 600 diffractometer using CuKα-emission in the angular range 3–90° (2θ) with a scanning step of 0.01° and a recording rate of 5°/min. The surface morphologies of PG-T system, PGB1-T system, and 1,2,4-triazole in powder form were analyzed with an environmental scanning electron microscope type Quanta 200 at 25kV with secondary electrons in low vacuum.

3.2. Synthesis of Benzoxazole-2′-yl-mercapto-acetic Acid Hydrazide (Compound I)

It was obtained by treating benzoxazol-2′-yl-mercapto-acetic acid ethyl ester with 98% hydrazine hydrate in anhydrous ethanol at room temperature.

3.3. General Procedure for Synthesis of 1-(Benzoxazole-2′-yl-mercapto-acetyl)-4-aryl-thiosemicarbazide (Compounds II–VII)

A total of 0.005 moles of benzoxazole-2′-yl-mercapto-acetic acid hydrazide (I) dissolved in 30 mL absolute methyl alcohol was treated with 0.005 moles of aromatic isothiocyanate in 5 mL anhydrous methanol. The mixture was refluxed for 2 h. During heating, a crystalline precipitate appeared and became more and more abundant once the reaction was complete. After cooling, the precipitate was filtered and washed with anhydrous ethyl ether. Purification was carried out by recrystallization from anhydrous methanol.

1-(Benzoxazole-2′-yl-mercapto-acetyl)-4-phenyl-thiosemicarbazide (Compound II), Physical state: White, crystalline powder; M$_p$ = 182–183 °C. FT-IR (KBr,ν, cm^{-1}): 2917, 3150 (NH); 1670 (C=O); 1400 (CH$_2$); 1145 (C=S); 755 (monosubstituted benzene nucleus); 700 (C-S).

1-(Benzoxazole-2′-yl-mercapto-acetyl)-4-(p-tolyl)-tiosemicarbazide (Compound III), Physical state: White-ivory powder, acicular crystals; M$_p$ = 163–164 °C. FT-IR (KBr,ν, cm^{-1}): 2880, 3096 (NH); 1709 (C=O); 1424 (CH$_2$); 720 (C-S); 750 (para-disubstituted benzene nucleus). ^{1}H-NMR (DMSO-d_6, 400 MHz, δ ppm): 2.11 (t, 3H, CH$_3$); 4.39 (s, 2H, CH$_2$); 6.95–6.98 (d, 2H, CHAr); 7.13–7.18 (d, 2H, CHAr); 7.57–7.63 (d, 2H, CHAr); 7.76–7.79 (d, 2H, CHAr); 9.86 (s, 1H, NHCO); 10.19 (s, 1H, NH); 10.76 (s, 1H, NH).

1-(Benzoxazole-2′-yl-mercapto-acetyl)-4-(p-methoxytolyl) thiosemicarbazide (Compound IV), Physical state: White, crystalline powder; M$_p$ = 186–188 °C. FT-IR (KBr,ν, cm^{-1}): 2918, 3096 (NH); 1623 (C=O); 1492 (CH$_2$); 1239 (C=S); 789 (monosubstituted benzene nucleus); 749 (C-S). ^{1}H-NMR (DMSO-d_6, 400 MHz, δ ppm): 3.38 (t, 3H, OCH$_3$); 4.38 (s, 2H, CH$_2$); 6.09–6.11 (d, 2H, CHAr); 7.11–7.13 (d, 2H, CHAr); 7.41–7.43 (d, 2H, CHAr); 7.84–7.92 (d, 2H, CHAr); 8.86 (s, 1H, NHCO); 10.26 (s, 1H, NH); 10.86 (s, 1H, NH).

1-(Benzoxazole-2′-yl-mercapto-acetyl)-4-(p-chlorophenyl) thiosemicarbazide (Compound V), Physical state: White-ivory, crystalline powder; M$_p$ = 147–149 °C. FT-IR (KBr,ν, cm^{-1}): 3096 (NH); 1620 (C=O); 1482 (CH$_2$); 1249 (C=S); 749 (para-disubstituted benzene nucleus); 710 (C-S); 629 (C-Br). ^{1}H-NMR (DMSO-d_6, 400 MHz, δ ppm): 4.27 (d, 2H, CH$_2$); 7.32–7.35 (d, 2H, CHAr); 7.38–7.40 (d, 2H, CHAr); 7.52–7.56 (d, 2H, CHAr); 7.65–7.67 (d, 2H, CHAr); 9.67 (s, 1H, NHCO); 9.90 (s, 1H, NH); 10.49 (s, 1H, NH).

1-(Benzoxazole-2′-yl-mercapto-acetyl)-4-(p-chlorophenyl)-thiosemicarbazide (Compound VI), Physical state: White-ivory, crystalline powder; M$_p$ = 150–151 °C. FT-IR (KBr,ν, cm^{-1}): 3080, 3124 (NH); 1620 (C=O); 1498 (CH$_2$); 1250 (C=S); 725 (C-Cl); 708 (C-S); 680 (para-disubstituted benzene nucleus). ^{1}H-NMR (DMSO-d_6, 400 MHz, δ ppm): 4.23 (d, 2H, CH$_2$); 6.92–7.04 (d, 2H, CHAr); 7.29–7.32 (d, 2H, CHAr); 7.39–7.41 (d, 2H, CHAr); 8.77 (s, 1H, NHCO); 10.11 (s, 1H, NH); 10.85 (s, 1H, NH).

1-(Benzoxazole-2′-yl-mercapto-acetyl)-4-(p-iodophenyl)-thiosemicarbazide (Compound VII). Physical state: White-yellow, crystalline powder; M$_p$ = 172–179 °C. FT-IR (KBr,ν, cm^{-1}): 3097, 3140 (NH); 1620 (C=O); 1490 (CH$_2$); 1120 (C=S); 785 (para-disubstituted benzene nucleus); 712 (C-S); 630 (C-I). ^{1}H-NMR (DMSO-d_6, 400 MHz, δ ppm): 4.25 (d, 2H, CH$_2$); 6.91–7.03 (d,

2H, CHAr); 7.30–7.31 (d, 2H, CHAr); 7.40–7.42 (d, 2H, CHAr); 7.66–7.69 (d, 2H, CHAr); 8.74 (s, 1H, NHCO); 10.10 (s, 1H, NH); 10.31 (s, 1H, NH).

3.4. General Procedure for Synthesis of 1-(Benzoxazole-2′-yl-mercapto-methyl)-5-(aryl-amino)-1,3,4,thiadiazoles (Compounds VIII–XIII)

A total of 6 mL of concentrated sulfuric acid were added under stirring to 0.005 moles of 1-(benzoxazole-2′-yl-mercapto-acetyl)-4-aryl-thiosemicarbazide (compounds II–VII). The reaction mixture was stirred at room temperature for 45–50 min to complete the cyclization and then was poured on crushed ice when an abundant precipitate appeared. The mixture was neutralized with ammonium hydroxide, and, after 2 h, the microcrystals were filtered in vacuum and washed with distilled water until the washing water reached pH = 7. Then, the obtained compounds were dried in vacuum oven at 55–60 °C and were purified by recrystallization from ethyl alcohol.

2-(Benzoxazole-2′-yl-mercapto-methyl)-5-(phenyl-amino)-1,3,4-thiadiazole (Compound VIII), Physical state: White-yellow, crystalline powder; M_p = 194–196 °C. FT-IR (KBr,ν, cm^{-1}): 2945, 3256 (NH); 1496 (CH$_2$); 1454 (N=C-S); 1401, 1535 (thiadiazole nucleus) 1090 (C-S-C); 785, 815 (para-disubstituted benzene nucleus); 750 (C-S). ^{1}H-NMR (DMSO-d_6, 400 MHz, δ ppm): 4.26 (s, 2H, CH$_2$); 6.91 (t, 1H, CHAr); 6.98–7.00 (d, 2H, CHAr); 7.46–7.49 (d, 2H, CHAr); 8.35 (d, 2H, CHAr); 8.71–8.72 (d, 2H, CHAr); 10.48 (s, 1H, NH).

2-(Benzoxazole-2′-yl-mercapto-methyl)-5-(tolyl-amino)-1,3,4-thiadiazole (Compound IX), Physical state: Brown-red, amorphous powder; M_p = 154–156 °C. FT-IR (KBr,ν, cm^{-1}): 2945 (NH); 1480 (CH$_2$); 1450 (N=C-S); 1448, 1517 (thiadiazole nucleus); 1070 (C-S-C); 828 (para-disubstituted benzene nucleus); 730 (C-S). ^{1}H-NMR (DMSO-d_6, 400 MHz, δ ppm): 2.29 (t, 3H, CH$_3$); 4.49 (s, 2H, CH$_2$); 7.36–7.38 (d, 2H, CHAr); 7.66–7.69 (d, 2H, CHAr); 8.21–8.23 (d, 2H, CHAr); 8.39–8.42 (d, 2H, CHAr); 10.21 (s, 1H, NH).

2-(Benzoxazole-2′-yl-mercapto-methyl)-5-(p-methoxyphenyl-amino)-1,3,4-thiadiazole (Compound X), Physical state: Brown, crystalline powder; M_p = 116–118 °C. FT-IR (KBr,ν, cm^{-1}): 2500, 3000 (NH); 1475 (CH$_2$); 1438 (N=C-S); 1243, 1615 (thiadiazole nucleus); 1068 (C-S-C); 830 (para-disubstituted benzene nucleus); 710 (C-S). ^{1}H-NMR (DMSO-d_6, 400 MHz), δ ppm: 3.38 (t, 3H, OCH$_3$); 4.53 (s, 2H, CH$_2$); 7.31–7.34 (d, 2H, CHAr); 7.53–7.56 (d, 2H, CHAr); 8.50 (d, 2H, CHAr); 8.86 (d, 2H, CHAr); 10.37 (s, 1H, NH).

2-(Benzoxazole-2′-yl-mercapto-methyl)-5-(p-bromophenyl-amino)-1,3,4-thiadiazole (Compound XI), Physical state: Brown, crystalline powder; M_p = 197–197°C. FT-IR (KBr,ν, cm^{-1}): 2880, 2905 (NH); 1480 (CH$_2$); 1449 (N=C-S); 1240, 1518 (thiadiazole nucleus); 1070 (C-S-C); 828 (para-disubstituted benzene nucleus); 750 (C-Br). ^{1}H-NMR (DMSO-d_6, 400 MHz), δ ppm: 4.49 (s, 2H, CH$_2$); 7.21-7.23 (d, 2H, CHAr); 7.47-7.51 (d, 2H, CHAr); 8.19-8.21 (d, 2H, CHAr); 8.33-8.35 (d, 2H, CHAr); 10.98 (s, 1H, NH).

2-(Benzoxazole-2′-yl-mercapto-methyl)-5-(p-chlorophenyl-amino)-1,3,4-thiadiazole (Compound XII), Physical state: Brown-white, crystalline powder; M_p = 201–203 °C. FT-IR (KBr,ν, cm^{-1}): 3318 (NH); 1475 (CH$_2$); 1450 (N=C-S); 1240, 1518 (thiadiazole nucleus); 1071 (C-S-C); 830 (para-disubstituted benzene nucleus); 755 (C-Cl). 1H-NMR (DMSO-d_6, 400 MHz), δ ppm: 4.32 (s, 2H, CH$_2$); 7.17–7.19 (d, 2H, CHAr); 7.39–7.42 (d, 2H, CHAr); 8.22–8.24 (d, 2H, CHAr); 8.54–8.57 (d, 2H, CHAr); 10.31 (s, 1H, NH).

2-(Benzoxazole-2′-yl-mercapto-methyl)-5-(p-iodophenyl-amino)-1,3,4-thiadiazole (Compound XIII), Physical state: Brown, crystalline powder; M_p = 187 °C. FT-IR (KBr,ν, cm^{-1}): 2880, 2918 (NH); 1478 (CH$_2$); 1462 (N=C-S); 1438, 1580 (thiadiazole nucleus); 1070 (C-S-C); 825 (para-disubstituted benzene nucleus); 760 (C-I). ^{1}H-NMR (DMSO-d_6, 400 MHz), δ ppm: 4.25 (s, 2H, CH$_2$); 7.28–7.32 (d, 2H, CHAr); 7.40–7.42 (d, 2H, CHAr); 8.16–8.18 (d, 2H, CHAr); 8.47–8.50 (d, 2H, CHAr); 10.27 (s, 1H, NH).

3.5. General Procedure for Synthesis of 3-(Benzoxazole-2′-yl-mercapto-methyl)-4-aryl-5mercapto-1,2,4-triazoles (Compounds XIV–XIX)

A total of 0.0027 moles of 1-(Benzoxazole-2′-yl-mercapto-acetyl)-4-aryl-thiosemicarbazide (II-VII) were treated with 20 mL of 2N sodium hydroxide solution at room temperature. Then, the reaction mixture was heated under reflux for 60 min. After that, the mixture was cooled, diluted with distilled water (*v/v*), and treated with a diluted solution of hydrochloric acid (1:1) to pH = 4.5. The precipitates [mercapto-1,2,4-triazole (compounds XIV–XIX) were filtered, washed on filter with 500 mL of distilled water, and finally dried. After recrystallization from boiling ethyl alcohol, the finished products were crystalline.

3-(Benzoxazole-2′-yl-mercapto-methyl)-4-phenyl-5-mercapto-1,2,4-triazoles (Compound XIV), Physical state: White, crystalline powder; M_p = 239–241 °C. FT-IR (KBr,ν, cm^{-1}): 3095 (NH); 1622 (C=N); 1490 (C=S); 820 (monosubstituted benzene nucleus); 785 (S-CH$_2$). ^{1}H-NMR (DMSO-d_6, 400 MHz), δ ppm: 4.78 (s, 2H, CH$_2$); 6.99–7.01 (d, 2H, CHAr); 7.13–7.15 (d, 2H, CHAr); 7.22 (t, 1H, CHAr); 14.06 (s, 1H, NH).

3-(Benzoxazole-2′-yl-mercapto-methyl)-4-(p-tolyl)-5-mercapto-1,2,4-triazole (Compound XV), Physical state: White-yellow, crystalline powder; M_p = 198–200 °C. FT-IR (KBr,ν, cm^{-1}): 3036 (NH); 1623 (C=N); 1492 (C=S); 898 (para-disubstituted benzene nucleus); 782 (S-CH$_2$). ^{1}H-NMR (DMSO-d_6, 400 MHz), δ ppm: 2.34 (t, 3H, CH$_3$); 4.51 (s, 2H, CH$_2$); 7.07–7.09 (d, 2H, CHAr); 7.28–7.30 (d, 2H, CHAr); 7.51–7.53 (d, 2H, CHAr); 14.04 (s, 1H, NH).

3-(Benzoxazole-2′-yl-mercapto-methyl)-4-(p-methoxyphenyl)-5-mercapto-1,2,4-triazole (Compound XVI), Physical state: White-ivory, crystalline powder; M_p = 213–215 °C. FT-IR (KBr,ν, cm^{-1}): 3100 (NH); 1628 (C=N); 1492 (C=S); 837 (para-disubstituted benzene nucleus); 783 (S-CH$_2$). ^{1}H-NMR (DMSO-d_6, 400 MHz), δ ppm: 3.46 (t, 3H, OCH$_3$); 4.29 (s, 2H, CH$_2$); 7.09–7.11 (d, 2H, CHAr); 7.25–7.27 (d, 2H, CHAr); 7.53–7.55 (d, 2H, CHAr); 14.09 (s, 1H, NH).

3-(Benzoxazole-2′-yl-mercapto-methyl)-4-(p-bromoyphenyl)-5-mercapto-1,2,4-triazole (Compound XVII), Physical state: Brown-red, crystalline powder; M_p = 202–204 °C. FT-IR (KBr,ν, cm^{-1}): 3328 (NH); 1617 (C=N); 1494 (C=S); 914 (para-disubstituted benzene nucleus); 780 (S-CH$_2$). ^{1}H-NMR (DMSO-d6, 400 MHz), δ ppm: 4.17 (s, 2H, CH$_2$); 7.20–7.23 (d, 2H, CHAr); 7.47–7.50 (d, 2H, CHAr); 7.75–7.77 (d, 2H, CHAr); 14.21 (s, 1H, NH).

3-(Benzoxazole-2′-yl-mercapto-methyl)-4-(p-chloroyphenyl)-5-mercapto-1,2,4-triazole (Compound XVIII), Physical state: White-ivory, crystalline powder; M_p = 189–191 °C. FT-IR (KBr,ν, cm^{-1}): 2894 (NH); 1615 (C=N); 1493 (C=S); 899 (para-disubstituted benzene nucleus); 765 (S-CH$_2$); 746 (c-Cl). ^{1}H-NMR (DMSO-d_6, 400 MHz), δ ppm: 4.64 (s, 2H, CH$_2$); 7.31–7.33 (d, 2H, CHAr); 7.42–7.44 (d, 2H, CHAr); 7.73–7.75 (d, 2H, CHAr); 14.29 (s, 1H, NH).

3-(Benzoxazole-2′-yl-mercapto-methyl)-4-(p-iodoyphenyl)-5-mercapto-1,2,4-triazole (Compound XIX), Physical state: Brown-red, crystalline powder; M_p = 222–224 °C. FT-IR (KBr,ν, cm^{-1}): 3038 (NH); 1614 (C=N); 1495 (C=S); 915 (para-disubstituted benzene nucleus); 770 (S-CH$_2$); 748 (C-I). ^{1}H-NMR (DMSO-d_6, 400 MHz), δ ppm: 4.23 (s, 2H, CH$_2$); 7.35–7.37 (d, 2H, CHAr); 7.42–7.45 (d, 2H, CHAr); 7.59–7.61 (d, 2H, CHAr); 14.33 (s, 1H, NH).

3.6. Antibacterial Activity

The microbial strains (*Staphylococcus aureus* (ATCC-2593), *Bacillus subtilis* (ATCC-6638), *Bacillus cereus* (ATCC-10876), *Salmonella entiritidis* (P-1131) and *Escherichia coli* (ATCC-25922)) were grown on Mueller–Hinton agar, with incubation at 37 °C for 48 h. Previously, the tested substances were weighted and dissolved in dimethylsulphoxide (DMSO) to prepare the solutions with the following concentrations: 1 mg/mL, 0.5 mg/mL, and 0.25 mg/mL culture medium. The solutions thus prepared were included in 100 mL of culture medium, previously agarized, melted, and then homogenized. In parallel, the control sample was prepared consisting of glucose agar. The culture media were then distributed in the test tubes and sterilized for 20 min at 120 °C. The bacterial cultures were prepared according

to the manufacture recommendations, using suspensions with a concentration of about $5.2 \cdot 10^7$ CFU/mL.

3.7. Immobilization of 1,2,4-Triazole

Immobilization of the 1,2,4-triazole was performed as follows: 0.2 g powder of PG and PGB1 copolymers were introduced into 50 mL conical flasks over which 20 mL of 1,2,4-triazole solution was added ($C_{1,2,4\text{-triazole}} = 3.6 \times 10^{-4}$ — 15×10^{-3} g/mL). Then, the samples were placed in a thermostated water-bath shaker (Memmert MOO/M01, Schwabach, Germany) and shaken at 180 strokes/minute until equilibrium was reached. The 1,2,4-triazole immobilization studies on PG and PGB1 copolymers were performed at different temperatures: 25, 30, and 35 °C and for different contact times. The conical flasks were removed from the water-bath shaker, and the copolymers were centrifuged at 78 RCF for 10 min. Then, the samples were separated by filtration, and the amount of 1,2,4-triazole immobilized on PG and PGB1 copolymers was determined by UV-VIS spectrophotometry (SPEKOL 1300 spectrophotometer, Analytik Jena, Jena, Germany) at a wavelength of 226 nm, based on a calibration curve. The retained amount of 1,2,4-triazole was calculated by the difference between 1,2,4-triazole concentration in the supernatant before and after sorption process.

The amount of immobilized 1,2,4-triazole was calculated using the following equation:

$$q_e = \frac{(C_0 - C_e) \cdot V}{W} \qquad (12)$$

where q_e is the amount of 1,2,4-triazole immobilized onto PG and PGB1 copolymers (mg/g), C_0 is the initial 1,2,4-triazole concentration (mg/mL), C_e is the equilibrium 1,2,4-triazole concentration (mg/mL), V is the volume of 1,2,4-triazole solution (mL), and W is the amount of copolymers. PG and PGB1 copolymers are in the form of powder consisting of irregularly shaped particles.

3.8. Release of 1,2,4-triazole

In vitro 1,2,4-triazole release studies were performed by immersing the PG-T and PGB1-T systems (0.1 g) in 10 mL of simulated gastric fluids of pH = 1.2 for 2 h at 37 °C. The samples were placed in a thermostated water-bath shaker under gentle stirring (50 strokes/minute). Samples (1 μL) of supernatant solution were collected at different time intervals using a microsyringe and then analyzed spectrophotometrically at a wavelength of 226 nm, using a UV-VIS spectrophotometer (Nanodrop ND 100, Wilmington, DE, USA). The amount of 1,2,4-triazole released was determined using the calibration curve.

4. Conclusions

The 2-mercapto-benzoxazole molecule was used to achieve a selective support for some heterocycles with 1,3,4-thiadiazole and 1,2,4-triazole structure, respectively. The addition reaction of benzoxazolyl-2-mercapto-acetic acid hydrazide to aromatic isothiocyanantes was used to obtain a new series of acyl-thiosemicarbazides (compounds II–VII). Applying the cyclization reaction, the 4-substituted acyl-thiosemicarbazides were converted in acid medium into thiadiazole derivatives with benzoxazole residue in the molecule (compounds VIII–XIII) and in basic medium in mercapto-triazole-3,4-disubstituted (compounds XIV–XIX). All new compounds were characterized using elemental and spectral analysis (FT-IR and ^{1}H-NMR). Among the active principles synthesized, 3-(benzoxazole-2′-yl-mercapto-methyl)-4-(p-methoxyphenyl)-5-mercapto-1,2,4 triazole was chosen to be immobilized onto a polymeric support due to its biological properties. The antimicrobial studies have shown that 1,2,4 triazole presents very good antimicrobial activities against several microbial strains, such as *Escherichia coli*, *Salmonella enteritidis*, and *Bacillus subtilis* compared to 1,3,4-thiadiazoles that show good antimicrobial activity against *Staphylococcus aureus*.

Two polymeric supports were used for the immobilization of 1,2,4-triazole derivative (compound XVI): grafted copolymer and grafted copolymer carrying betaine moieties based on gellan and N-vinyl imidazole, which were chosen due to the biocompatibility of the polysaccharide as well as of the polymer/grafts generated by the vinyl monomer and betaine function.

To describe the interactions that occur in sorption processes between 1,2,4-triazole and PG and PGB1 copolymers, Langmuir, Freundlich, and Dubinin–Radushkevich model isotherms were used. Kinetic sorption studies conclude that the Lagergren model best describes the experimental data and confirm that the sorption of 1,2,4-triazole on the grafting copolymers is physical in nature.

The thermodynamic study completed by the kinetic one led to the conclusion that the sorption process of 1,2,4-triazole on the betainized copolymer is more intense than in the case of the grafted copolymer only. The sorption process of 1,2,4-triazole is spontaneous and favored by the increase of temperature. The release of 1,2,4-triazole from polymeric supports proceeds through a complex mechanism controlled by both swelling and diffusion processes. Similar to the results obtained in case of immobilization of the cefotaxime sodium salt, these results confirm the potential of the grafted copolymer with betaine structure as a candidate for developing sustained/controlled drug delivery systems.

References

1. Laraia, L.; Robke, L.; Waldmann, H. Bioactive compound collections: From design to target identification. *Chem* **2018**, *4*, 705–730. [CrossRef]
2. Liechty, W.B.; Kryscio, D.R.; Slaughter, B.V.; Peppas, N.A. Polymers for drug delivery systems. *Annu. Rev. Chem. Biomol. Eng.* **2010**, *1*, 149–173. [CrossRef] [PubMed]
3. Farshori, N.N.; Banday, M.R.; Ahmad, A.; Khan, A.U.; Rauf, A. Synthesis, characterization and in vitro antimicrobial activities of 5-alkenyl/hydroxyalkenyl-2-phenylamine-1,3,4-oxadiazoles and thiadiazoles. *Bioorg. Med. Chem. Lett.* **2010**, *20*, 1933–1938. [CrossRef] [PubMed]
4. Pintilie, O.; Profire, L.; Sunel, V.; Popa, M.; Pui, A. Synthesis and antimicrobial activity of some new 1,3,4-thiadiazole and 1,2,4-triazole compounds having a D,L-methionine moiety. *Molecules* **2007**, *12*, 103–113. [CrossRef] [PubMed]
5. Kadi, A.A.; El-Brollosy, N.R.; Al-Deeb, O.A.; Habib, E.E.; Ibrahim, T.M.; El-Emam, A.A. Synthesis, antimicrobial and antiinflammatory activities of novel 2-(1-adamantyl)-5-substituted-1,3,4-oxadiazoles and 2-(1-adamantylomini)-5-substituted-1,3,4-thiadiazoles. *Eur. J. Med. Chem.* **2007**, *42*, 235–242. [CrossRef] [PubMed]
6. Tan, C.X.; Shi, Y.X.; Weng, J.Q.; Liu, X.H.; Zhao, W.G.; Li, B.J. Synthesis and antifungal activity of novel 1,2,4-triazole derivatives containing 1,2,3-thiadiazole moiety. *J. Heterocycl. Chem.* **2014**, *51*, 690–694. [CrossRef]
7. Klip, N.T.; Capan, G.; Gursoy, A.; Uzun, M.; Satana, D. Synthesis, structure and antifungal evaluation of some novel 1,2,4-triazolylmercaptoacetyl thiosemicarbazide and 1,2,4-triazolylmercaptomethyl-1,3,4 thiadiazole analogs. *J. Enzyme Inhib. Med. Chem.* **2010**, *25*, 126–131. [CrossRef] [PubMed]
8. Xu, J.; Cao, Y.; Zhang, J.; Yu, S.; Zou, Y.; Chai, X.; Wu, Q.; Zhang, D.; Jiang, Y.; Sun, Q. Design, synthesis and antifugal activities of novel 1,2,4-triazole derivatives. *Eur. J. Med. Chem.* **2011**, *46*, 3142–3148. [CrossRef] [PubMed]
9. Gupta, D.; Jain, D.K. Synthesis, antifungal and antibacterial activity of novel 1,2,4-triazole derivatives. *J. Adv. Pharm. Technol. Res.* **2015**, *6*, 141–146. [CrossRef] [PubMed]

10. Solak, N.; Rollas, S. Synthesis and antituberculosis activity of 2-(aryl/alkylamino)-5-(4-aminophenyl)-1,3,4-thiadiazoles and their Schiff bases. *Arkivoc* **2006**, *12*, 173–181. [CrossRef]

11. El-Reedy, A.A.M.; Soliman, N.K. Synthesis, biological activity and molecular modeling study of novel 1,2,4 triazolo[4,3-b] [1,2,4,5] tetrazines and 1,2,4-triazolo [4,3-b] [1,2,4] triazines. *Sci. Rep.* **2020**, *10*, 6137. [CrossRef] [PubMed]

12. Amir, M.; Kumar, H.; Javed, S.A. Condensed bridgehead nitrogen heterocyclic system: Synthesis and pharmacological activities of 1,2,4-triazolo-[3,4-b]-1,3,4-thiadiazole derivatives of ibuprofen and biphenyl-4-yloxy acetic acid. *Eur. J. Med. Chem.* **2008**, *43*, 2056–2066. [CrossRef] [PubMed]

13. Kumar, H.; Javed, S.A.; Khan, S.A.; Amir, M. 1,3,4-Oxadiazole/thiadiazole and 1,2,4-triazole derivatives of bisphenyl-4-yloxy acetic acid: Synthesis and preliminary evaluation of biological properties. *Eur. J. Med. Chem.* **2008**, *43*, 2688–2698. [CrossRef] [PubMed]

14. Salgin-Goksen, U.; Gokhan-Kelekci, N.; Goktas, O.; Koysa, Y.; Kilic, E.; Isik, S.; Aktay, G.; Ozalp, M. 1-Acylthiosemicarbazides, 1,2,4-triazole-5(4H)-thiones, 1,3,4-thiadiazoles and hydrazones containing 5-methyl-2-benzoxazolinones: Synthesis, analgesic-antiinflammatory and antimicrobial activities. *Bioorg. Med. Chem.* **2007**, *15*, 5738–5751. [CrossRef] [PubMed]

15. Amir, M.; Khan, M.S.Y.; Zaman, M.S. Synthesis, characterization and biological activities of substituted oxadiazole, triazole, thiadiazole and 4-thiazolidinone derivatives. *Indian J. Chem.* **2004**, *43B*, 2189–2194. [CrossRef]

16. Clerici, F.; Pocar, D.; Guido, M.; Loche, A.; Perlini, V.; Brufani, M. Synthesis of 2-amino-5-sulfanyl-1,3,4-thiadiazole derivatives and evaluation of their antidepressant and anxiolytic activity. *J. Med. Chem.* **2001**, *44*, 931–936. [CrossRef] [PubMed]

17. Cressier, D.; Prouillac, C.; Hernandez, P.; Amourette, C.; Diserbo, M.; Lion, C.; Rima, G. Synthesis, antioxidant properties and radioprotective effects ofnew benzothiazoles and thiadiazoles. *Bioorg. Med. Chem.* **2009**, *17*, 5275–5284. [CrossRef] [PubMed]

18. Sharma, P.C.; Bansal, K.K.; Sharma, A.; Sharma, D.; Deep, A. Thiazole-containing compounds as therapeutic targets for cancer therapy. *Eur. J. Med. Chem.* **2020**, *188*, 112016. [CrossRef] [PubMed]

19. Gomha, S.M.; Abdelhamid, A.O.; Abdelrehem, N.A.; Kandeel, S.M. Efficient synthesis of new benzofuran-based thiazoles and investigation of their cytotoxic activity against human breast carcinoma cell lines. *J. Heterocycl. Chem* **2018**, *55*, 995–1001. [CrossRef]

20. Padmavathi, V.; Reddy, G.S.; Padmaja, A.; Kondaiah, P.; Shazia, A. Synthesis, antimicrobial and cytotoxic activities of 1,3,4-oxadiazoles, 1,3,4-thiadiazoles and 1,2,4-triazoles. *Eur. J. Med. Chem.* **2009**, *44*, 2106–2112. [CrossRef] [PubMed]

21. Gomha, S.M.; Kheder, N.A.; Abdelaziz, M.R.; Mabkhot, Y.N.; Alhajoj, A.M. A facile synthesis and anticancer activity of some novel thiazoles carrying 1,3,4-thiadiazole moiety. *Chem. Cent. J.* **2017**, *11*, 25. [CrossRef] [PubMed]

22. Choritos, G.; Trafalis, D.T.; Delezis, P.; Potamitis, C.; Sarli, V.; Zoumpoulakis, P.; Camoutsis, C. Synthesis and anticancer activity of novel 3,6-disubstituted 1,2,4-triazolo-[3,4-b]-1,3,4-thiadiazole derivatives. *Arabian J. Chem.* **2019**, *12*, 4784–4794. [CrossRef]

23. Jain, A.K.; Sharma, S.; Vaidya, A.; Ravichandran, V.; Agrawal, R.K. 1,3,4-Thiadiazole and itas derivatives: A review on recent progress in biological activities. *Chem. Biol. Drug Des.* **2013**, *81*, 557–576. [CrossRef] [PubMed]

24. Chen, J.; Sun, X.Y.; Chai, K.Y.; Lee, J.S.; Song, M.S.; Quan, Z.S. Synthesis and anticonvulsant evaluation of 4-(4-alkoxylphenyl)-3-ethyl-4H-1,2,4-triazoles as open-chain analogues of 7-alkoxyl-4,5-dihydro[1,2,4]triazolo[4,3-a]quinolines. *Bioorg. Med. Chem.* **2007**, *15*, 6775–6781. [CrossRef] [PubMed]

25. Datar, P.A.; Deokule, T.A. Development of thiadiazole as an antidiabetic agent-A review. *Mini Rev. Med. Chem.* **2014**, *14*, 136–153. [CrossRef] [PubMed]

26. Van der Nieuwendijk, A.M.C.H.; Pietra, D.; Heitman, L.; Goblyos, A.; IJzerman, A.P. Synthesis and biological evaluation of 2,3,5 substituted [1,2,4] thiadiazoles as allosteric modulators of adenosine receptors. *J. Med. Chem.* **2004**, *47*, 663–672. [CrossRef]

27. Leung-Toung, R.; Wodzinka, J.; Li, W.; Lowrie, J.; Kukreja, R.; Desilets, D.; Karimian, K.; Tam, T.F. 1,2,4 thiadiazole: A novel Cathepsin B inhibitor. *Bioorg. Med. Chem.* **2003**, *11*, 5529–5537. [CrossRef] [PubMed]

28. Sayeed, I.B.; Vishnuvardhan, M.V.P.S.; Nagarajan, A.; Kantevari, S.; Kamal, A. Imidazopyridine linked triazoles as tubulin inhibitors, effectively triggering apoptosis in lung cancer cell line. *Bioorg. Chem.* **2018**, *80*, 714–720. [CrossRef] [PubMed]

29. Desai, T.; Desai, V.; Shingade, S. In-vitro Anti-cancer assay and apoptotic cell pathway of newly synthesized benzaxazole-N-heterocyclic hybrids as potent tyrosine kinase inhibitors. *Bioorg. Chem.* **2020**, *94*, 103382. [CrossRef] [PubMed]

30. Yuan, X.; Yang, Q.; Liu, T.; Li, K.; Liu, Y.; Zhu, C.; Zhang, Z.; Li, L.; Zhang, C.; Xie, M.; et al. Design, synthesis and in vitro evaluation of 6-amide-2-aryl benzoxazole/benzimidazole derivatives against tumor cells by inhibiting VEGFR-2 kinase. *Eur. J. Med. Chem.* **2019**, *179*, 147–165. [CrossRef] [PubMed]

31. Belal, A.; Abdelgawad, M.A. New benzothiazole/benzoxazole-pyrazole hybrids with potential as COX inhibitors: Design, synthesis and anticancer activity evaluation. *Res. Chem. Intermed.* **2017**, *43*, 3859–3872. [CrossRef]

32. Padalkar, V.S.; Borse, B.N.; Gupta, V.D.; Phatangare, K.R.; Patil, V.S.; Umape, P.G.; Sekar, N. Synthesis and antimicrobial activity of novel 2-substituted benzimidazole, benzoxazole and benzothiazole derivatives. *Arab. J. Chem.* **2016**, *9*, S1125–S1130. [CrossRef]

33. Seth, K.; Garg, S.K.; Kumar, R.; Purohit, P.; Meena, V.S.; Goyal, R.; Banerjee, U.C.; Chakraborti, A.K. 2-(2-Arylphenyl)benzoxazole as a novel anti-inflammatory scaffold: Synthesis and biological evaluation. *ACS Med. Chem. Lett.* **2014**, *5*, 512–516. [CrossRef] [PubMed]

34. Sheng, C.; Xu, H.; Wang, W.; Cao, Y.; Dong, G.; Wang, S.; Che, X.; Ji, H.; Miao, Z.; Yao, J.; et al. Design, synthesis and antifungal activity of isosteric analogues of benzoheterocyclic N-myristoyltransferase inhibitors. *Eur. J. Med. Chem.* **2010**, *45*, 3531–3540. [CrossRef] [PubMed]

35. Ryu, S.K.; Lee, R.Y.; Kim, N.Y.; Kim, Y.H.; Song, A.L. Synthesis and antifungal activity of benzo[d]oxazole-4,7-diones. *Bioorg. Med. Chem. Lett.* **2009**, *19*, 5924–5926. [CrossRef]
36. Jauhari, P.K.; Bhavani, A.; Varalwar, S.; Singhal, K.; Raj, P. Synthesis of some novel 2-substituted benzoxazoles as anticancer, antifugal and antimicrobial agents. *Med. Chem. Res.* **2008**, *17*, 412–424. [CrossRef]
37. Haider, S.; Alam, M.S.; Hamid, H.; Shafi, S.; Nargotra, A.; Mahajan, P.; Nazreen, S.; Kalle, A.M.; Kharbanda, C.; Ali, Y.; et al. Synthesis of novel 1,2,3-triazole based benzoxazolinones: Their TNF-β based molecular docking with in-vivo anti-inflammatory, antinociceptive activities and ulcerogenic risk evaluation. *Eur. J. Med. Chem.* **2013**, *70*, 579–588. [CrossRef] [PubMed]
38. Kakkar, S.; Kumar, S.; Narasimhan, B.; Lim, S.M.; Ramasamy, K.; Mani, V.; Shah, S.A.A. Design, synthesis and biological potential of heterocyclic benzoxazole scaffolds as promising antimicrobial and anticancer agents. *Chem. Cent. J.* **2018**, *12*, 96. [CrossRef] [PubMed]
39. Duroux, R.; Renault, N.; Cuelho, J.E.; Agouridas, L.; Blum, D.; Lopes, L.V.; Melnyk, P.; Yous, S. Design, synthesis and evaluation of 2-aryl benzoxazoles as promising hit for the A_{2A} receptor. *J. Enzyme Inhib. Med. Chem.* **2017**, *32*, 850–864. [CrossRef] [PubMed]
40. Kale, M.; Chavan, V. Exploration of the biological potential of benzoxazoles: An overview. *Mini Rev. Org. Chem.* **2019**, *16*, 111–126. [CrossRef]
41. Padmavathi, V.; Kumara, C.P.; Venkatesh, B.C.; Padmaja, A. Synthesis and antimicrobial activity of amido linked pyrrolyl and pyrazolyl-oxazoles, thiazoles and imidazoles. *Eur. J. Med. Chem.* **2011**, *46*, 5317–5326. [CrossRef] [PubMed]
42. Racovita, S.; Baranov, N.; Macsim, A.M.; Lionte, C.; Cheptea, C.; Sunel, V.; Popa, M.; Vasiliu, S.; Desbrieres, J. New grafted copolymers carrying betaine units based on gellan and N-vinylimidazole as precursors for design of drug delivery systems. *Molecules* **2020**, *25*, 5451. [CrossRef] [PubMed]
43. Aparaschivei, R.; Holban, M.; Sunel, V.; Popa, M.; Desbrieres, J. Synthesis and characterization of new heterocyclic compounds with potential antituberculosis activity and their immobilization on polymer supports. *Cellul. Chem. Technol.* **2012**, *46*, 301–306.
44. Cheptea, C.; Sunel, V.; Desbrieres, J.; Popa, M. Synthesis and antimicrobial activity of new derivatives of 1,3,4-thiadiazoles and 1,2,4-triazoles with 5-nitroindazole as support. *J. Heterocycl. Chem.* **2013**, *50*, 366–372. [CrossRef]
45. Moise, M.; Sunel, V.; Profire, L.; Popa, M.; Desbrieres, J.; Peptu, C. 1,4-Disubstituted thiosemicarbazides with potential tuberculostatic action. *Bull. Inst. Polit. Iasi.* **2009**, *55*, 57–64.
46. Moise, M.; Sunel, V.; Profire, L.; Popa, M.; Desbrieres, J.; Peptu, C. Synthesis and biological activity of some new 1,3,4-thiadiazole and 1,2,4-triazole compounds containing a phenylalanine moiety. *Molecules* **2009**, *14*, 2621–2631. [CrossRef] [PubMed]
47. Hussain, S.; Sharma, J.; Amir, M. Synthesis and antimicrobial activities of 1,2,4-triazole and 1,3,4-thiadiazole derivatives of 5-amino-2-hydroxybenzoic acid. *J. Chem.* **2008**, *5*, 963–968. [CrossRef]
48. Cheptea, C.; Sunel, V.; Morosanu, C.; Dorohoi, D.O. Derivatives of 1,2,4-triazole-3,4-disubstituted based on aminoaxids with potential biological activity. *Rev. Chim.* **2020**, *71*, 211–221. [CrossRef]
49. Langmuir, I. The adsorption of gases on plane surface of glass, mica and platinum. *J. Am. Chem. Soc.* **1918**, *40*, 1361–1368. [CrossRef]
50. Weber, T.W.; Chakravot, R.K. Pore and solid diffusion models for fixed bed adsorbents. *AiChE J.* **1974**, *20*, 228–238. [CrossRef]
51. Foo, K.Y.; Hameed, B.H. Insights into the modeling of adsorption isotherm systems. *Chem. Eng. J.* **2010**, *156*, 2–10. [CrossRef]
52. Freundlich, H.M.F. Over the adsorption in solution. *J. Phys. Chem.* **1906**, *57*, 385–470.
53. Dubinin, M.M.; Zaverina, E.D.; Radushkevich, L.V. Sorption and structure of active carbons. I. Adsorption of organic vapors. *Zhurnal Fizicheskoi Khimii.* **1947**, *21*, 1351–1362.
54. Chabani, M.; Amrane, A.; Bensmaili, A. Kinetic modelling of the adsorption of nitrates by ion exchange resin. *Chem. Eng. J.* **2006**, *125*, 111–117. [CrossRef]
55. Yu, Y.; Zhuang, Y.Y.; Wang, Z.H.; Qiu, M.Q. Adsorption of water-soluble dyes onto modified resin. *Chemosphere* **2004**, *54*, 425–430. [CrossRef]
56. Rodriguez, A.; Garcia, J.; Ovejero, G.; Mestanza, M. Adsorption of anionic and cationic dyes on activated carbon from aqueous solutions: Equilibrium and kinetics. *J. Hazard. Mat.* **2009**, *172*, 1311–1320. [CrossRef]
57. Cigu, T.A.; Vasiliu, S.; Racovita, S.; Lionte, C.; Sunel, V.; Popa, M.; Cheptea, C. Adsorpion and release studies of new cephalosporin from chitosan-g-poly(glycidyl methacrylate) microparticles. *Eur. Polym. J.* **2016**, *82*, 132–156. [CrossRef]
58. Lagergren, S.; Svenska, B.K. Zur theorie der sogenannten adsorption geloester stoffe. *Kungl. Sven. Vetenskapsakad. Handl.* **1898**, *24*, 1–3.
59. Ho, Y.S.; McKay, G. The kinetics of sorption of basic dyes from aqueous solutions by sphagnum moss peat. *Can. J. Chem. Eng.* **1998**, *76*, 822–827. [CrossRef]
60. Higuchi, W.I. Diffusional models useful in biopharmaceutics. *J. Pharm. Sci.* **1967**, *56*, 315–324. [CrossRef]
61. Korsmeyer, R.W.; Gurny, R.; Doelker, E.; Buri, P.; Peppas, N.A. Mechanisms of solute release from porous hydrophilic polymers. *Int. J. Pharm.* **1983**, *15*, 25–35. [CrossRef]